REVIEW

Check for updates

Evaluation of photoanode materials used in biophotovoltaic systems for renewable energy generation†

Maira Anam, [ID] *[a] Helena I. Gomes, [ID] [a] Geoffrey Rivers, [ID] [b] Rachel L. Gomes [ID] [a] and Ricky Wildman [ID] [b]

Biological photovoltaic (BPV) cells are living solar panels capable of producing clean energy by extracting electrons from sunlight (in daytime) and stored carbon in microbial cells (during the night or on cloudy days), irrespective of the organic substrate supply. The physicochemical properties of anode surfaces harbouring microbial communities in BPV systems influence the electrochemical charge transfer rate at the electrode. Hence, these properties play a significant role in regulating the kinetics of metabolic reactions in the biotic compartment while providing an electron transfer path. Various electrically conductive materials have been explored as solid-state anodes to improve the power output and economic viability of BPV systems. However, the current systems still suffer from low power density due to electrodes' electrochemical limitations and a lack of systematic optimization of the device. This review provides a comprehensive insight into the recent developments in different anode materials, their dimensional structure, and their impact on the performance of BPV systems in the last two decades. Moreover, the existing limitations of electrode materials in BPV systems are summarized, and outlooks for future anode advancements are foreseen.

1. Introduction

Global energy consumption has increased substantially, and our current energy infrastructure is primarily dependent on fossil fuels.[1] As a result, it is most likely that the associated rapid greenhouse gas emission from rapid economic development will instigate severe climate emergency and biosphere damage.[2] Although the understanding of the precise impact of such anthropogenic interferences on the ecosystem is evolving, without carbon-free energy technology, policy response, and socioeconomic interventions, climate change seems inevitable within the next 50 years.[3] The one way to reduce the reliance of the world economy on fossil energy is through carbon-neutral fuel sources. Sunlight, an abundant and inexhaustible energy source, is considered a future sustainable energy choice to balance the development and environment of our planet.[4] Theoretically, sunlight has far more potential than any other renewable energy sources available on Earth, with 5×10^4 EJ [5]

[a]Food Water Waste Research Group, Faculty of Engineering, University of Nottingham, University Park, Nottingham, NG7 2RD, UK. E-mail: Maira.Anam1@nottingham.ac.uk; Helena.Gomes1@nottingham.ac.uk; rachel.gomes@nottingham.ac.uk; Tel: +44 (0)1158467244; +44 (0)1158468883

[b]Centre for Additive Manufacturing, Faculty of Engineering, University of Nottingham, Jubilee Campus, Nottingham, NG8 1BB, UK. E-mail: Geoffrey.rivers@nottingham.ac.uk; Ricky.Wildman@nottingham.ac.uk; Tel: +44 (0)7384291225; +44 (0)1158466893

† Electronic supplementary information (ESI) available. See DOI: 10.1039/d1se00396h

available for harvest and capture annually.[6] However, at present photovoltaic (PV) solar cells are the only major technology available in the market for solar energy conversion.[7] Photovoltaic devices use semiconductor materials to generate electricity from photons through the photovoltaic effect, and only when the light source is available.[8] The power conversion efficiency (PCE) of commercially available solar cells is around $18 \pm 2\%$ at peak solar intensity (1 kW m^{-2}) and AM 1.5 spectral distribution.[9] Considering we are exclusively focusing on PCE here, not the total integrated expense report of a PV system including renewal requirements, infrastructure, energy input and environmental concomitance, technology with better efficiency simply may not be perfect to implement.[9] We are approaching the theoretical efficiency limits of PVs.[8] Life cycle assessment of synthetic PV devices has revealed some major shortcomings, including high upfront cost for installation, maintenance, operation, land, water and capital;[10] insufficient disposal facilities for used batteries[11] and the use of precious metallic or toxic dye components in panel fabrication.[12,13] In addition to technical barriers such as energy losses due to failure (4.26%) and inefficiencies (22.34–27.58%), there are other operational issues such as daily variation in sunlight availability necessitating energy storage, inadequate infrastructure, and climate, economic and institutional hindrances, which means that PV cells would best be accompanied by additional renewable energy generation methods.[14] Thus, environmentally friendly and low-cost alternatives to PVs that resolve these technical

barriers are immensely desirable. Compared to solid-state photovoltaic devices, natural photosynthetic solar energy conversion systems store energy in a diverse array of organic products, from light driven carbon dioxide reduction, which are later used for cell maintenance.[15] During natural photosynthesis, sunlight is trapped by oxygenic photosynthetic organisms to catalyze a series of charge separation events, splitting water into oxygen, protons, and electrons while sequestering carbon dioxide. An artificial photosynthesis system spatially integrates a biocatalyst to capture solar energy in a more energy efficient way for oxygen reduction and simultaneously generates electricity by transferring some of the resultant electrons to an anode.[16] Both systems are different in the light absorption range, power conversion efficiency, and energy storage capabilities. Unlike PVs, photosynthetic organisms intrinsically store the energy that is produced, in the form of consumable biomass which is available for power extraction even under dark conditions; analogous to a PV with integrated storage capacity. Although the PCE is clearly in the favour of PV systems, to attain sustainable energy for future both need to be applied.[9]

Biological photovoltaics (BPVs) are emerging systems that concurrently exploit the advantages of photovoltaics and bio-electrochemical cells to generate electricity by harvesting solar energy without relying on any exogenous supply of reducing equivalents (Fig. 1).[17] Numerous cyanobacterial[18] and green algal[19] biofilms have been used in BPV systems to harness solar energy. Similarly, purified subcellular photosynthetic apparatus such as the photosynthesis reaction centre (photosystem II) extracted from thermophilic cyanobacteria[20,21] and thylakoid membranes isolated from spinach leaves[22,23] can be attached to electron-accepting electrodes in BPV systems. In the last two decades, BPV systems have attracted increasing research interest,[24,25] due to their relatively simple fabrication, inexpensive and self-sustainable catalyst materials, and environmental friendliness.[26] Moreover, BPV systems have the potential to generate electricity continuously throughout the day and night

as well, unlike solid-state PVs.[27] The key aspect of this device is that it generates electricity-convertible radicals without the need for a human-supplied source of reducing agents to fuel the reaction. In oxygenic photosynthesis, cells absorb carbon dioxide from the atmosphere while water is used as the substrate for photolysis to generate electrons, protons, and oxygen.[17] The exact process can be exploited in BPVs to generate electricity, and in the presence of sunlight, photons' energy is used to drive charge separation within photosystems and high energy electrons are generated. Some of these excited electrons are routed by the cellular machinery to the metabolite NADPH in nature, which is later used to provide energy for carbon fixation.[16,28] Even when not illuminated, stored carbon nutrients produced during illuminated periods are oxidized by the respiratory metabolism of microbes, producing an electron radical source available for anode capture.[27,28] Transfer of these excited electrons from the microbial cells on an anode to an external circuit can occur via either direct or indirect transfer mechanisms. It is these excited electrons and possibly redox-capable high energy metabolites that are the source of current in BESs, although the exact transfer mechanisms are still under investigation.[27]

Other light-driven bioelectrochemical systems (BESs) (Fig. 2) should be distinguished from BPV systems depending on the biocatalyst, source of reducing equivalents, and reaction type. For example, photosynthetic microbial fuel cells (photoMFCs) require sunlight and an external source of organic matter to generate electricity from anoxygenic microorganism's metabolism.[29,30]

Another example is complex photosynthetic microbial fuel cells (complex pMFCs), where oxygenic photosynthetic organisms harvest solar energy, sequestering carbon temporarily as organic biomass, which is subsequently metabolized by heterotrophic bacteria to generate electricity.[31] Other systems such as organic photovoltaic devices (OPVs) and dye-sensitized solar cells (DSSCs) use biological pigments extracted from plant leaves (e.g.
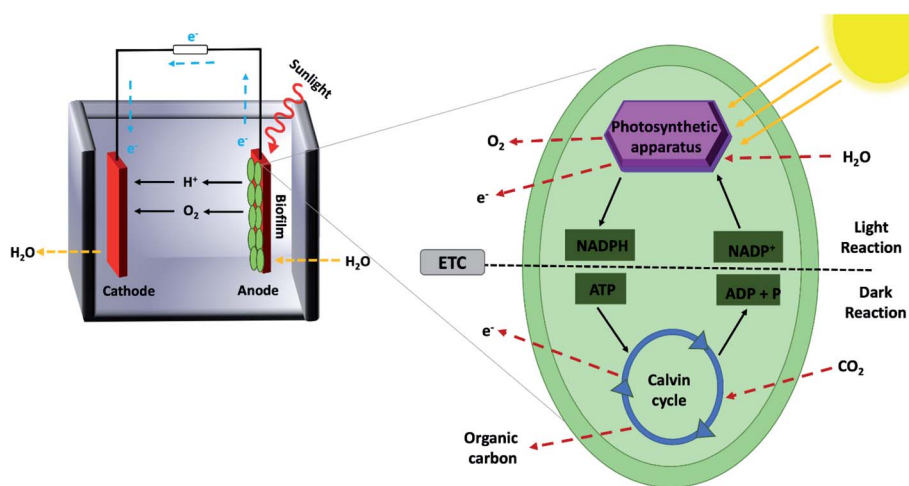

Fig. 1 Schematic illustration of a cellular biophotovoltaic (BPV) system and components involved in light–dependent electron generation. Abbreviations: H_2O, water; O_2, oxygen; H^+, proton; e^-, electron; CO_2, carbon dioxide; NADPH, nicotinamide adenine dinucleotide phosphate; ATP, adenosine triphosphate; ADP, adenosine diphosphate; p, inorganic phosphate.
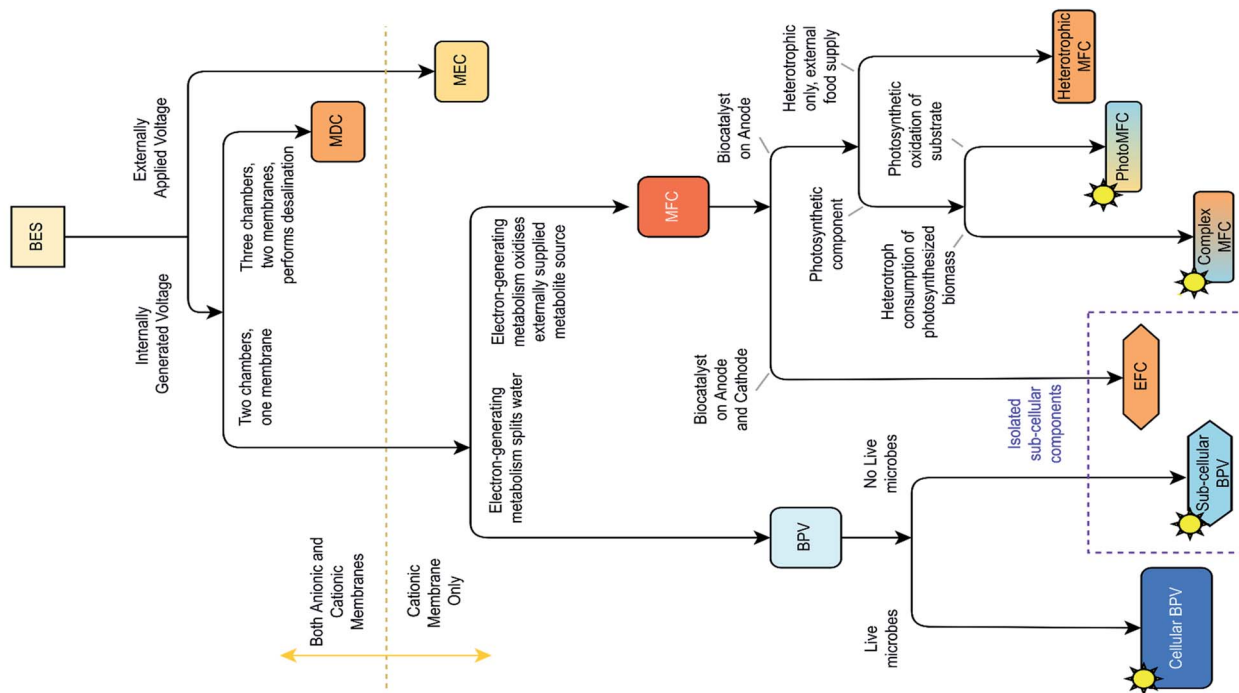
Fig. 2 Classification of bioelectrochemical systems (BESs), based on differences in structure and function, adapted from ref. 16. MEC, microbial electrosynthesis cell; MDC, microbial desalination cell; MFC, microbial fuel cell; BPV, biophotovoltaic system; photoMFC, photosynthetic microbial fuel cell; EFC, enzymatic fuel cell.

carotenoids, chlorophyll)[32] or use synthetic dyes (e.g. carbol fuchsin, aniline blue, etc.)[33,34] to harvest light. However, these systems require a supply of sacrificial electron-donor reactants.[35,36] There are other BESs, defined by their mode of application, such as enzymatic fuel cells (EFCs) employing a single enzyme or an aggregate of pure redox enzymes (oxidoreductases) extracted from living cells as catalysts at the anode,[37,38] microbial electrosynthesis cells (MECs) integrating fuel (H_2) production at the cathode powered by organic matter oxidation at the anode,[39] and microbial desalination cells (MSCs) that allow electricity production and simultaneous water desalination through inserting an anion exchange membrane along with a cation exchange membrane.[40] These are not closely related to BPV systems and, therefore, will not be discussed further.

BPV systems are complex devices that rely on their components' dynamic electrochemical, biological, and physical–chemical interactions to achieve maximum performance.[16] A BPV system's operation involves a complex interplay between metabolic and electrochemical reactions, including the transfer of electrons from the cells to the anode. The known extracellular electron transfer mechanisms include the metal reducing pathway from *Shewanella oneidensis* MR-1;[41] porin like outer membrane cytochrome (omcS) filament structures or electrically conductive pili (pilA) from *Geobacter sulfurreducens*;[42,43] and redox endogenous mediators (e.g., flavins and phenazines) produced by a number of bacteria. However, the phototrophic equivalence of these aforementioned mechanisms observed in electrogenic heterotrophs has not been identified in *Synechocystis* sp. To the best of our knowledge there is no experimental evidence for soluble redox active compounds produced for intracellular electron transfer being used by cyanobacteria for extracellular electron transfer. Externally added mediators such as potassium ferricyanide when used in BPVs are known to improve the voltage response but could be toxic to microbes and even the environment at high concentration, making them unfeasible for long-term operation.[44] Understanding the relative contribution of these intracellular electron transfer mechanisms and whether they are the only options to supply reducing equivalents in cyanobacterial exoelectrogenic activity would account for improved current production.[16]

The progress of BPV systems in the last few decades has been limited to the standardization of the experimental setup and systematic optimization (Fig. 3).[16] However, to achieve the full potential of BPV system power output and successfully commercialise the application, it will be necessary to improve operational efficiency, which requires further investigation of the underlying process mechanisms, manufacturing parameters, and property relationships within these devices.[16] Previous literature has already highlighted the developments of key aspects of BPV performance.[16,24] For example, they outlined the impact of various operating parameters on the BPV performance and progress made towards scaling up BPV systems (Fig. 3). They have also identified the suboptimal power limitations of BPV systems based on reactor configuration (which can be either single or double chamber) or on the mode of electron transfer with or without artificial mediators.[45] Compared to conventional BESs, BPV systems have an additional requirement of optical transparency for their anodes to allow light penetration deep within biofilms; however, the
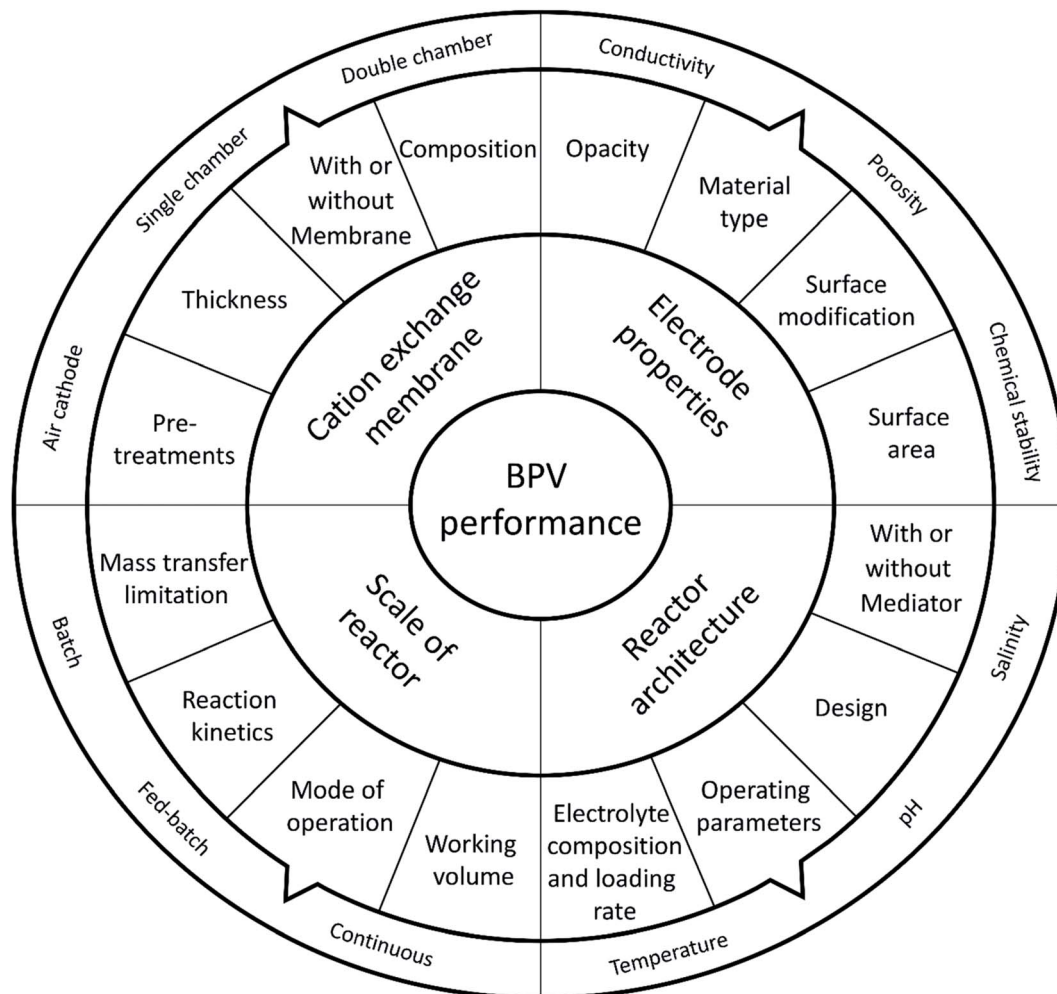
Fig. 3   Important parameters for developing high performance biophotovoltaic systems, adapted from ref. 48.

restricted material options and lack of fabrication techniques have hampered the engineering of improvements.

Several efficiency limiting factors of BPVs are intrinsic to the fundamental structure and organization of the multijunction tandem photosynthetic apparatus and a major re-engineering would be essential in order to improve.[9] Other straightforward efficiency improvement strategies would include structural adjustment of organisms and optimization of some system variables such as growth conditions, anode material properties and design, efficiency of the photosynthetic organisms,[46] efficiency of the proton exchange membrane,[45] light intensity and spectra,[47] and chemistry of the electrolyte solution.[47] Electrochemical losses are mainly responsible for the insignificant power output reported so far with BPV systems compared to their theoretically estimated ideal cell voltage.[16] Among the above system parameters, anode materials and design are most urgently in need of optimization: conventional anode materials often hinder the redox homeostasis potential of photosynthetic microorganisms, thus impeding electron exchange processes between cells;[25] improved understanding and optimization of this ubiquitous component would have a wide-ranging impact for all BPV systems.

This review focuses on the recent progress in various electrode materials and the architecture employed in biophotovoltaic systems, including those composed of metal, carbon forms, transparent conducting oxides, and composite electrodes. The electrochemical characteristics and surface chemistry of the electrodes exhibiting improved current generation are discussed, concerning their influences on BPV system efficiency and photocurrent density. The reported achievements of power conversion for various anodes and cell designs are standardized and used to compare their relative capabilities. This review also summarises the rational design and selection of biophotovoltaic cell electrode materials in the literature, discussing these with regard to improving current generation and identifying limitations of electrode designs.

2.   Ideal electrodes

The influence of the anode on BES overall performance has been previously summarized,[49] but it is also a crucial factor in governing the bioelectrical properties of BPV systems. BPVs are emerging forms of BESs and exclusively include photosynthetic microorganisms in their anodic chamber while their

heterotrophic counterpart harnesses electrons by oxidizing organic matter.[16] Considering the limited studies (37 between year 1964 and 2008) published on the BPV topic,[16] MFCs with far more established literature are often referred to, to find relevant information about the abiotic performance scenarios. One needs to keep in mind that all these devices summarized in Fig. 2 are BESs with similar design and use anodes only distinguished based on their separate reductive processes and the respective requirements that result from that. For example, light penetration for BPVs and organic matter supply for MFCs. As long as we are aware of these differences, we can refer to MFC data without a conflict. The integration of photosynthetic redox agents into a BPV system requires a spatially organised bio-interface of immobilised cells, or enzymes, on a conductive support to establish efficient electron transfer pathways for photocurrent generation. Hence, the anode functions as the collector of reducing equivalents diffusing from photoactive biomaterials. The anode surface's dual functionality is to be a conductor for electron transfer and a microbial community carrier. An ideal anode must have good electrical properties and surface roughness to favour biofilm growth.[24] In addition to electrode surface morphology, the biocatalytic activity of the attached biofilm is determined by the parameters affecting surface energy, resistance exerted by the biofilm's extracellular polymeric substances, biocompatibility, communication of living cells with the electrode surface, and the nature of target microbial species (cell surface charge and size).[50] The essential properties of an electrode material for BPV systems are high electrical conductivity and long-term electrochemical stability within the range of applied electric potentials.

2.1 Transparency

A fundamental property for the enhancement of a BPV system's electrodes in theory is that light should be able to penetrate within the anode structure to illuminate any embedded photosynthetic microorganisms.[51] Transparent electrodes would allow light that is not absorbed by a microbial biofilm to pass through the anode and cathode layers, allowing a layered BPV system design, potentially increasing energy production density.[52] While transparency might not be a necessity it is believed that BPVs could stand to benefit from it more than any other system.

2.2 Electrical conductivity

The electrons released from microbial metabolism are collected by the anode and routed toward the cathode through an external circuit to participate in oxygen reduction. Low ionic conductance at the anode, resulting in high impedance, is one of the fundamental limitations in enabling high power density of a BPV system. An electrode surface with high electrical conductivity amplifies the microbial electron transfer rate and consequently the power produced by maintaining a continuous supply of terminal electron acceptors, where an electrically inactive electrode resists the transfer of electrons resulting from microbial metabolism. There are strong chances of microbial oxidation on an anode surface with high potential indicating its

superior electrochemical properties. The high internal resistance of an anode is often attributed to its physical (low intrinsic conductivity of the material, poor interfacial contact) and biological properties (loss of contact between the biological/inorganic interfaces, ineffective long-range electron transfer through the biofilm).[53] Nevertheless, a key factor is achieving low interfacial resistance at the biofilm–electrode contact point, to improve the efficiency of extracellular electron capture.[54]

2.3 Chemical stability

In any BES, the electrodes are in direct contact with the aqueous electrolyte matrix and are continuously subjected to physical, chemical, and enzymatic variations. Anode materials that may be susceptible to side-reactions under the wide range of conditions might limit their performance in real applications. Chemical reaction of the anode material under the localized strong oxidising or reducing conditions present during operation may cause decay of the electrode surface, reducing interface quality and compromising performance. Additionally, every reaction with the anode material represents a radical electron that the anode failed to capture and route to the electrical circuit. Therefore, the discovery of a robust anode with stable chemistry in a wide array of conditions (particularly ionic strength, chemical composition, pH and applied voltage) is of increasing importance for BPV systems.[55]

2.4 Biocompatibility

In general, biocompatibility is the degree to which a material or surface does not cause harm to an organism or a system of organisms under study. In the context of BPV systems, the electrode material is considered biocompatible if it is non-toxic, easy to manipulate, dimensionally stable and not known to induce host survival response. For the anodic reaction that is based on microbial photolysis of water, if cells are to be cultivated on the electrode as a biofilm, then the biocatalyst interactions with the electrode material should be considered.[56] Poor anode–microbe interactions can lead to activation losses during BPV system operation and subsequently, low current densities.[57] Materials used for the anode must demonstrate a good affinity for host microbial cells for their growth and facilitate bacterial adhesion on their surfaces.[58] Carbon, graphite, and metal oxides are the commonly employed electrically conductive materials as anodes in BPV systems due to their lower toxicity towards anode biofilms.[24]

2.5 Surface area

The limited surface area of anodes has largely constrained the performance of BPV systems for industrial implementation, as the net ohmic losses are proportional to the electrochemically active surface area and electrical resistance of the electrode. Increasing the active surface area while maintaining the same working volume overcomes the internal resistance and increases the cell loading.[59] Increasing the anode's specific area improves the mass transfer of nutrients and reaction kinetics of the heterogeneous processes, subsequently maximizing the power densities of a BPV system.[60] Alongside this, the impacts

of electrode surface charge and chemistry (hydrophilic or hydrophobic) on biofilm colonization were reported for photo-bioelectrocatalytic fuel cells.[61] Electrode properties such as porosity, surface area, and roughness can influence the resulting biofilm's distribution, cell density, and stability. An interconnected porous electrode structure serves as a scaffold for microbial attachment leading to a more stable biofilm under strong shear flow conditions but clogged pores in the interior of the electrode would then lead to mass transport limitations.[62] On the other hand, biofilms that develop on a smooth planar anode surface are more conducive to mass transfer and homogeneously exposed to bulk electrolyte. However, they are easily damaged and prone to detachment, particularly when exposed to shear forces from electrolyte flow.[63]

2.6 Cost and accessibility

Another crucial aspect of scaling up BPV systems is that the electrode material should be abundantly available and low cost. Besides these basic requirements, using electrode materials in ready supply will increase their widespread application in fundamental bioelectrochemical studies.[55] Expensive components are mainly responsible for limiting the commercial application of BPV systems. The ideal anode material should be affordable, sustainable, and readily available. One of the easiest ways to reduce the capital cost of a BPV system is to develop low-cost materials, allowing optimization studies to use high specific surface area electrode designs, and to better investigate the efficiency mechanisms.[64]

3. Anode materials used in BPVs

Experimental studies have been focused on engineering approaches to improve BPV system operations, including the use of different construction materials[24] and novel configurations or design of BPV systems.[65] Two of the goals of investigating new electrode materials are facilitating bacterial adhesion and increasing electron transfer from the bacteria into the substrate and associated conductive circuits. Good adhesion of microbes to an anode is critical for power generation in a BPV system. Considerable research has been entirely focused on the chemical surface modification of electrodes and performance evaluation of conventional electrode materials, rather than optimising electrode design and electrochemical properties due to the lack of economically efficient production processes. Controlled electrode fabrication, correlated to the resulting electrical conductivity, could be a potential tool to investigate improvements to the system efficiency and determine the best configuration for immobilised bioactive reducing components (e.g. algal cells, photosystems or thylakoid membrane).[66]

A considerable body of research has focused on optimising electrode materials in BPV system configurations, focusing on increasing the rate of electron transfer to favour the reaction kinetics and power output of the system.[18] The selection criteria for electrode design have progressed over the last four decades, prioritizing the increase in electrochemically available specific surface area. So far, three different categories of anodic materials have been investigated in mediator-free BPV systems. Type I consists of inorganic metallic electrodes, one of the early-stage anodes in BPV systems, representing a good compromise between the requirements of stability, conductivity, and biocompatibility. Improving on this, type II is carbon electrodes, exhibiting improved surface roughness for denser loading of photosynthetic biofilms or isolated protein complexes. Type I and type II anodes are generally found in the fundamental studies of cyanobacterial species in BPV system setups in the literature. Recent advancements in electrode
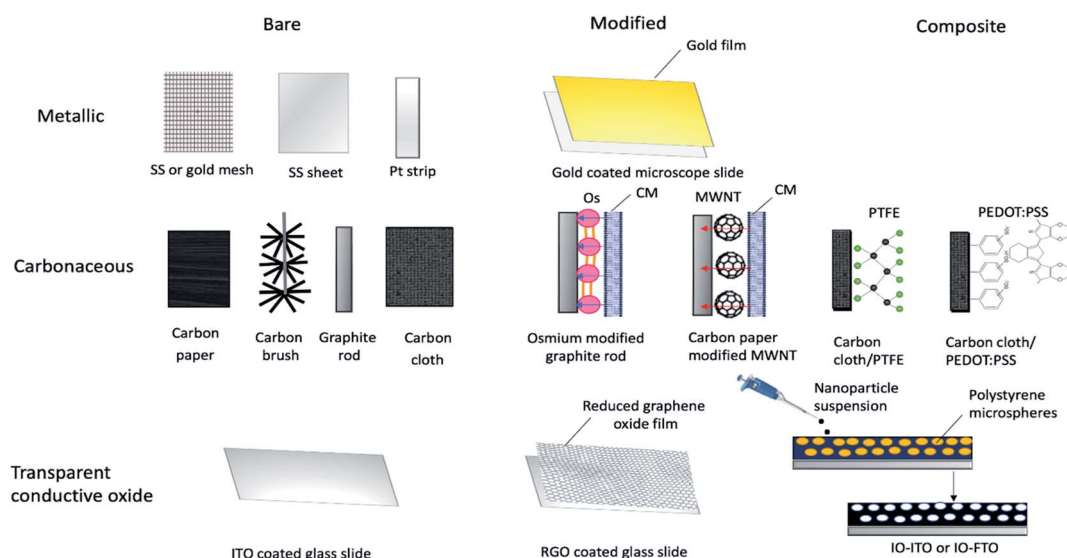

Fig. 4 Summary of various electrode configurations used in biophotovoltaic systems. Abbreviation: SS, stainless steel; Pt, platinum; Os, osmium; CM, cytoplasmic membrane; MWNT, multiwalled nanotube; PTFE, polytetrafluoroethylene; PEDOT:PSS, poly(3,4-ethylenedioxythiophene):polystyrene sulfonate; ITO, indium tin oxide; IO-ITO, inverse opal indium tin oxide; IO-FTO, inverse opal fluorine doped tin oxide.

design have developed type III: porous glass or ceramic anodes, which outperform all other tested material types in terms of current generation.[50,62] We will discuss studies using anodes from each of these categories, detailing first BPV research in specific and then BES research in general (Fig. 4).

3.1. Inorganic metallic anodes

Metallic anodes such as gold, platinum, nickel, silver, and stainless steel are commonly employed in BPV systems due to their superior physical, electrical and mechanical properties besides their stability while acting as a current collector[50] (Table 1). Moreover, these metals are characterised by their high chemical strength, isotropic outer atomic orbitals, abundant raw materials and well-established processing techniques, although this can come with high environmental costs. Depending on their chemistry and the local electrochemical environment, these materials may natively display either a metallic surface or a passivated oxide surface; a difference within this class may produce different biofilm adhesion responses, interfacial contact, and interfacial conductivity.

Beyond BPV systems, to date, the performance of various metal-based anodes has been analyzed in BESs. The resistivity and economic viability of different monolithic metals, such as copper, cobalt, silver, stainless steel, nickel, titanium, and gold, were investigated and compared to a standard electrode material, graphite as the anode in microbial fuel cells.[67] The results revealed a favourable power output and thick biofilm formation for all metal anodes except for cobalt and titanium. Despite the variety of metals available in market only a few appear to be biocompatible as BES anodes. Passive or noble metals (or alloys) which display electrochemically inert behaviour in the operational potential window of BESs are suitable as anode materials. Copper anodes delivered a maximum current density of 1.5 mA cm^{-2}, provided that many electrochemically active bacteria can overcome the antimicrobial oligodynamic effect of heavy metal ions.[67] Moreover, the net material cost for the fabrication of a 1 m^{-2} flat plate copper electrode with a thickness of up to 11 μm was also estimated to be significantly lower (0.53 USD per m^{-2}) than that for the most expensive graphite electrode (26 USD per m^{-2}).[67]

Platinum and gold belong to the transition metal group. These noble metals are directly used as anodes without any surface modification in fundamental BPV system research,[68–70] as metallic surfaces offer a high degree of electrochemical inertness and reversibility. An example is platinum strips, which have been proposed as anode materials for

Table 1 Performance of metallic anode materials in biophotovoltaic (BPV) systems[a]

Anode material	Anode configuration	Anode dimensions	Photosynthetic species	Reactor setup (type, temperature, electrolyte, mediator)	Light intensity	Maximum power density
Platinum (Fu et al., 2009)[68]	Plane	5 cm length, 0.5 cm width and 0.1 cm thickness	*Spirulina platensis*	Single chamber membrane-free photosynthetic microbial fuel cell, 28 °C to 30 °C, Zarrouk medium	30 μmol photons per m^2 s provided by a white fluorescent lamp	0.132 mW m^{-2}
Platinum (Fu et al., 2010)[69]	Plane	5 cm length, 0.5 cm width and 0.1 cm thickness	*Spirulina platensis*	Single chamber membrane-free photosynthetic microbial fuel cell, 30 °C, Zarrouk medium	30 μmol photons per m^2 s from a white fluorescent lamp	5 mW m^{-2}
Stainless steel (Bombelli et al., 2012)[50]	Plane	100×20 mm^{-2}	*Pseudanabaena limnetica*	Multi-channel mediator-free biophotovoltaic system, 22 ± 2 °C, BG-11 medium	Alternative 2 h light and dark cycle of a white fluorescent lamp at 36.72 μmol photons per m^2 s or 8 W m^{-2} intensity	5.05 mW m^{-2}
Gold (Lin et al., 2013)[70]	Mesh plate	5.2 cm diameter and 200 mesh	*Spirulina platensis*	Photosynthetic microbial fuel cell, 30 °C, Zarrouk medium	3×10^{-9} μmol photons per m^2 s from a white fluorescent lamp	10 mW m^{-2}
Gold (Samsonoff et al., 2014)[149]	Plane	Surface area: 225 mm^{-2}	*Synechococcus bacillaris*	Photosynthetic-plasmonic-voltaic cell	4.5 mW laser diode ($\lambda =$ 670 nm)	0.0057 mW m^{-2}
Stainless steel mesh (Bazdar et al., 2018)[73]	Mesh	Mesh size of 400, length of 70 cm, width of 3.5 cm, and apparent surface area 245 cm^{-2}, 3 L	*Chlorella vulgaris*	Photosynthetic microalgae microbial fuel cell, 25 ± 2 °C, modified BG-11 medium	70 μmol photons per m^2 s or 5000 lux from an 18 W fluorescent lamp	126 mW m^{-3}

[a] BG-11, blue green-11 medium; power density was calculated by normalizing the power output to the surface area of the anode; unit conversion for light intensity was performed according to the coefficient values of *Plant Growth Chamber Handbook*.[75]

photosynthetic microbial cells (structurally consistent with a BPV system, although reported under different nomenclature).[68,69] Similarly, the higher surface area of gold mesh plates allows a better electronic tuning between the biofilm and the conductive band, emphasizing the potential effectiveness of rational material selection in BPV system design.[70] A disadvantage of such electrodes is the additional cost which often limits the use of these electrodes in large technical systems.[67]

Compared to other expensive precious metals (*e.g.*, silver, gold, and platinum), stainless steel (SS) is an affordable iron-based alloy that possesses electric conductivity, excellent mechanical stability, good biocompatibility, and corrosion resistance.[71,72] Hence, stainless steel is a more frequently employed anode in the configuration of BPV systems.[67,73] The performance of SS as a bioanode has been systematically tested against other materials, namely carbon paper (CP), indium tin oxide (ITO) coated polyethylene terephthalate (PET), and glass coated with a conductive polymer (PANI) in BPV systems. SS achieved the highest voltage output (170.1 ± 3.9 mV) followed by ITO (143.3 ± 3.7 mV), PANI (70.3 ± 0.2 mV) and CP (35.1 ± 1.1 mV) under light conditions.[50] Contrary to what was expected, in this study surface roughness had little impact on the ratio of maximum dark and light power outputs, possibly because the experiments were performed under stagnant conditions allowing the cells to settle.

Stainless steel, an inexpensive base metal, has also drawn considerable attention as an alternative anode material in BESs, specifically when the objective is to customize anode shapes for large-scale applications at an affordable price.[71] However, SS as a bioanode has been criticized for undesirable interference of SS components with the microbial community, inevitable corrosion, and limited surface area due to a flat geometry.[74] In SS, a compact oxide layer is formed on the surface that acts as a passivation layer to prevent further oxidation.[67] Given that SS can easily be processed into various shapes and surface area is fundamentally a design issue, the shortcoming of limited surface area can be improved, for example by employing SS meshes similar to the gold meshes above.[71] The additional resistance of the passivating oxide layer and the subsequent irreversibility of the electron transfer, however, are major drawbacks of such electrodes.[67] The biocompatibility of a stainless-steel anode depends mainly on its composition. Toxic metal components of SS (such as chromium, nickel, and molybdenum) may negatively affect an anode's overall biocompatibility by imposing metal ion stress on microbial activities.[56,71] Similarly, a relatively chemically stable SS bioanode in ambient environmental media, such as water, steam, and air, is prone to corrosion under the electric field of a BES, which could negatively impact the microbial growth and performance efficiency.[76,77] Corroded stainless steel loses its ability to collect electrons and acts as a sacrificial anode supplying electrons.[56] For instance, stainless steel mesh (SSM) was used as the anode in a photosynthetic microalgae microbial fuel cell to establish the optimum illumination regimes for simultaneous electricity production from *Chlorella vulgaris* at the cathodic compartment.[73] The SSM structure ensures better hydrodynamics and provides a large surface area for microbial

attachment, thereby demonstrating a significant improvement in mass transfer efficiency and subsequently voltage output compared to the plain geometry.

The metallic electrodes that have been employed in BPV systems as anodes so far exhibit decent biocompatibility, stability, and conductivity.[67] However, there are some drawbacks such as inconsistent and limited photocurrent stemming from the cyanobacterial biofilm. Flat metallic anodes with simple planar geometries are some of the greatest challenges in pilot studies or where reproducible datasets are required.[72] Despite being relatively cheap, unmodified metals' poor biocompatibility diminishes the power output produced by bioanodes.[78] Another drawback is the minimal surface roughness of metal electrodes limiting the surface area for attachment of living cells.[24,67] The interfacial area of non-porous flat metal anodes is confined to the geometry's projected surface area, limiting microbial growth to the external surface. The fact that only microbial cells in direct contact with the electrode surface can actively participate in current generation may further contribute to a decrease in power density.[78] Moreover, the oxidative erosion, high internal impedance, and anti-static properties might retard the electron transfer, limiting its engineering application in long-term operations.[56,71] Metal corrosion observed alters the released electrons which are consumed to reduce metal ions, negatively impacting the growth of microbes on the anode surface in BESs.[56] Additionally, some metal ions released from the oxidation reaction in the electrolyte are toxic and impair the life cycle of microorganisms by disrupting enzymatic and cellular functions.[79] The complexity in moulding metal to electrodes with well-defined pores in which cells can grow also hampers the use of metal-based anodes in BPV systems.

3.2. Conventional carbon-based anodes

Carbonaceous materials are by far the most commonly used anodes in all types of BESs, including BPV systems, due to their several favourable features such as structural polymorphism, relatively inert electrochemistry, significant electrical conductivity, rich surface chemistry for redox reaction, and low cost (Table 2).[80] Carbon exists in a wide variety of forms including traditional materials (graphite, carbon cloth and carbon fibres) and various novel families of carbon-based materials (graphene, carbon nanotubes, and nanoporous materials) grouped according to their basic structure and hybridization.[81] Based on their exact chemical and aggregate structure, these closely related materials exhibit a high degree of variation in their physical and chemical properties, such as electrochemical charge transfer, conductivity, chemical reactivity, optical transmissivity, and thermal conductivity.[81] Several studies have illustrated the significance of different carbon electrode topologies and surface morphologies to establish an effective interface with immobilised microorganisms.[82,83] Various carbon forms with their unique properties and advanced electrochemical performance have overcome the initial limitation of introducing nano and micron sized structures in inorganic materials to facilitate biofilm growth and have rapidly emerged

Table 2 Performance of carbon-based anode materials in biophotovoltaic (BPV) systems[a]

Anode material	Anode configuration	Anode dimensions	Photosynthetic species	Reactor setup (type, temperature, electrolyte, mediator)	Light intensity	Maximum power density or current density
Carbon cloth (Thorne et al., 2011)[62]	Fibrous	Not mentioned, (0.35 mL min^{-1} electrolyte)	Chlorella vulgaris	Photo-microbial fuel cells, Bold basal medium with 3-fold nitrogen and vitamin, 2.5 mM ferricyanide	Low monochromatic light illumination of 12 W m^{-2} or 55.8 µmol photons per m^2 s at 652 nm	0.2 mW m^{-2}
Carbon paper (Bombelli et al., 2012)[50]	Flat	100 × 20 mm^{-2}	Pseudanabaena limnetica	Multi-channel mediator-free biophotovoltaic system, 22 ± 2 °C, BG-11 medium	2 h light (36.72 µmol photons per m^2 or 8 W m^2) and 2 h dark cycle	2.05 mW m^{-2}
Carbon fibre (Madiraju et al., 2012)[89]	Flat	0.05 × 0.03 m, surface area: 0.0015 m^{-2}, anode volume: 60 mL	Synechocystis sp. PCC6803	Two-chamber MFC, 21 °C, BG-11 medium	High intensity light (140 µmol photons per m^2 s or 10 000 lux) provided by a 60 W white light bulb	0.01 mW m^{-2}
Graphite (Raman et al., 2012)[105]	Flat	Total dimensions in length, width and height of the anodic chamber are 27, 11 and 8.5 cm; working volume: 500 mL	Chlamydomonas reinhardtii	Dual chamber photo microbial fuel cells, 25 °C, Tris acetate phosphate medium (pH 7)	12 h of light (21 µmol photons per m^2 s or 1500 lux) and 12 h of dark conditions	0.82 mW m^{-2}
Graphite (Lan et al., 2013)[107]	Flat	Total dimensions in length, width and height of the anodic chamber are 27, 11 and 8.5 cm; working volume: 500 mL	Chlamydomonas reinhardtii	Dual chamber photosynthetic microbial fuel cells, 25 °C, Tris acetate phosphate medium	Blue (450–495 nm) and red (620–750 nm) monochromatic LED lights of varying intensity: 100, 300, 600 and 900 lux	12.947 mW m^{-2} with blue light at 900 lux or 12.6 µmol photons per m^2 s intensity
Multi-walled carbon nanotubes on carbon paper (Sekar et al., 2014)[98]	Nanotubes	10 nm diameter × 1–2 µm length, geometric surface area of CP base: 0.0254 cm^{-2}	Fresh cultures of filamentous cyanobacteria: Nostoc sp. ATCC 27893 and Anabaena variabilis ATCC 29413	Photo-bio electrochemical cell, 25 ± 2 °C, BG-11 medium	12 : 12 h light-dark cycles illuminated using fluorescent lamps (80 µmol photons per m^2 s)	35 mW m^{-2}
Carbon cloth (Cereda et al., 2014)[90]	Fibrous	3 × 1 cm	Synechocystis sp. PCC6803	Mediator-free biophotovoltaic system, 22 °C, BG-11 medium, 5 mM ferricyanide	LH7 red LED light source (peak λ = 660 nm), light intensity: 110 µmol photons per m^2 s or 20 W m^{-2}	4 mA m^{-2}
Graphite plates (Huang et al., 2015)[106]	Flat	45.09 cm^{-2}, anodic volume: 70 mL	Chlamydomonas reinhardtii	Photo microbial fuel cell, 25 °C, Tris-acetate-phosphate liquid medium	4 h of light (~30 µmol photons per m^2 s) and 4 h of darkness	0.0084 mW m^{-2}
Carbon cloth (Wei et al., 2016)[150]	Fibrous	Anode chamber: 140 µL, flow rate of 1 L min^{-1}	Synechocystis sp. PCC 6803	Microfluidic bio-solar panel, 30 °C, BG-11 medium	12 h light/dark intervals under 4 fluorescent lamps Fluorescent lamps (80 µmol photons per m^2 s)	8 mW m^{-2}
Carbon paper modified with multi-walled	Nanotubes	10 nm diameter × 1–2 µm length, geometric surface				10 mA m^{-2}

Table 2 (Contd.)

Anode material	Anode configuration	Anode dimensions	Photosynthetic species	Reactor setup (type, temperature, electrolyte, mediator)	Light intensity	Maximum power density or current density
carbon nanotubes (Sekar et al., 2016)[100]		area of CP base: 0.0254 cm^{-2}	Synechococcus elongatus PCC 7942	Photo-bio electrochemical cells, 30 ± 2 °C, BG-11 medium		
Carbon cloth (Liu et al., 2017)[108]	Flat	Projected surface area: 0.07 cm^{-2}, 140 mL-sized anode chamber	Synechocystis sp. PCC 6803	Dual chamber miniaturized biological solar cell with an air cathode, 30 ± 2 °C, BG-11 medium	24 h cycle of 12 h light/12 h dark	16 mW m^{-2}
Carbon nanotubes (Sawa et al., 2017)[99]	Nanotubes	Total geometrical area of the anode is 12.5 cm^{-2}	Synechocystis sp. PCC 6803	A hybrid BPV system with an air cathode, 30 °C, BG-11 medium containing 3.6% (w/v) NaCl	White LED illumination (50 μmol photons per m^2 s)	0.38 mW m^{-2}
Carbon cloth (Wang et al., 2018)[85]	Flat	80 mm × 80 mm, volume of the anode chamber: 1000 mL	Marine algae (Chlorella)	Buffer-free photosynthetic microbial fuel cell	12 h under a 6 W fluorescent lamp	4.06 mW m^{-2}
Carbon felt (Li et al., 2019)[86]	Flat	6 cm × 6 cm, anodic volume: 200 mL	Chlorella vulgaris	Bubbling-type photosynthetic algae microbial fuel cell, 25 °C, BG-11 medium	Continuous illumination from a cool-white fluorescent lamp (light intensity: 49 μmol photons per m^2 s or 3500 lux)	1108.9 mW m^{-3}
Carbon brushes (Yang et al. 2019)[96]	Brushes	Height: 150 mm, diameter: 30 mm, working volume of the anode: 0.36 L	Algal raceway pond	Photosynthetic microbial fuel cell stack, 25 °C, anaerobically digested effluent from kitchen waste	100 μmol photons per m^2 s	2.34 W m^{-3}

[a] BG-11, blue green-11 medium; PBS, phosphate buffered saline; NaCl, sodium chloride; power density was calculated by normalizing the power output to the surface area of the anode; unit conversion for light intensity was performed according to the coefficient values of Plant Growth Chamber Handbook.[75]

as reliable alternatives in fuel cell technology.[84] Apart from nano-roughness providing favourable anchoring points for the biofilm growth by enhancing cell adhesion, a porous carbonaceous electrode might reduce the overall diffusion resistance for direct electron transfer. Representative examples of carbon anodes used in BPV systems are flexible and self-supported carbon cloth, paper, or felt featuring high micron-sized fibres and are given in Table 2.

3.2.1 Carbon. Carbon in the form of carbon paper, carbon mesh, carbon felt, and carbon cloth has been widely used as the anode in different BES designs with varied substrates and inoculums.[85,86] Carbon cloth (CC) is an electrically conducting material formed through the layering of arbitrarily arranged short carbon fibres throughout a two-dimensional sheet.[87,88] CC acted as a promising anode in several studies.[89,90] Carbon cloth woven through ultralight carbon fibre fabric displayed good properties when used as the bioanode in a light-driven mediator-free BPV system.[90] A positive correlation of photocurrent with light intensity from 0 to 10 W m^{-2} was observed with genetically modified *Synechocystis* sp. PCC6803, immobilized on a carbon cloth electrode.[90] Similarly, the chemically inert carbon fibres with their outstanding mechanical and electrical properties acted as an excellent base anode for microorganism growth and CO_2 sequestration (467 mmol m^{-3}) in a photosynthetic microbial fuel cell (photoMFC).[89] In a similar study, carbon gauze was embedded in a dilute algal cell suspension to overcome the extracellular membrane restrictions in harvesting electrons, and enhanced electrical connectivity of the electrode with algal cells was reported.[91]

Although CC has demonstrated promising results in BPV systems, untreated carbon cloth is hydrophobic and generally exhibits a relatively insignificant response to electroactive agents.[92] Moreover, the extreme operating temperature often accelerates the carbonization shrinkage, and hence, deteriorates the mechanical stability and electrical conductivity by altering the structural matrix of fibres and closing the pores.[88,92,93] To compensate for carbon cloth performance, considerable efforts have been devoted to modification approaches.[94] In this context, Wang and his colleagues proposed an aluminum-alloy mesh composite carbon cloth (AAMCC) material for a photo MFC, which provided a sizeable adhering surface and a low equivalent resistance for enhanced electrochemical performance with a maximum current density of 46.34 mA m^{-2}.[85]

Carbon fibres have been reported to produce a maximum power density of 6.7 mW m^{-3} under 10 000 lux illumination, while sequestered about 467 mmol m^{-3} CO_2.[89] Carbon brushes are primarily carbon fibre strands wound around conductive metal wires with a tapered tip, which offer high specific surface area, electrical conductivity, and low resistance along the fibre axis for BES application.[88] The chemically inert carbon brushes appear to have great advantages over other carbon-based anodes. In carbon brushes, fibres with micrometer or nanometer diameters can work in small volumes while retaining a large electrode surface area.[95] Hence, they have been widely used as an electrode in BPV system setups owing to their chemical stability, biocompatibility, and the ultra-small size of

the 3D structured fibres, which enables their use as a micro-electrode or perhaps even as a nanoelectrode.[88,96] Multiple carbon brushes were explored as an anode in a photo MFC for anaerobically digesting household kitchen waste effluent.[96]

Carbon nanotubes (CNTs) are comparatively a novel member of the carbon allotrope family with unique physical properties and advanced electrochemical performances.[97] The closed structure of multiwalled carbon nanotubes (MWNTs) is composed of concentric graphite tubules aligned with multiple layers of graphite sheets that provide promising geometric, mechanical, chemical, and electronic properties for electrochemical applications.[80,97] CNT-based anodes have been reported in several BPV system studies with various benefits, such as decreased over-potential, increased voltammetric output, negligible surface fouling and increased heterogeneous electron transfer rates.[98,99] For instance, carbon paper (CP) with MWNTs drop-cast on the surface was used as a bioanode in a photoelectrochemical cell; the CNT modified electrode established a direct extracellular electron transfer pathway for improved electricity production. The integrated CP/MWNT yields a maximum photocurrent density of 250 mA m^{-2} without any exogenous mediator.[98,100]

Another novel digitally printed MWNT anode on A4 copy paper was reported for BPV systems, which generated a sustained electrical current both under light and dark conditions to power a digital clock and an LED.[99] However, the presence of metallic, amorphous carbonaceous and nano graphitic impurities drastically influences its electrochemical properties, limiting its application in BPV systems. Therefore, additional washing processes are considered to remove the impurities and obtain CNTs with stable electrical characteristics.[80]

3.2.2 Graphite. Graphite, an allotropic form of carbon, exhibits high chemical stability against microbial degradation, low electrical resistance (high electrical conductivity), and biocompatibility.[78] Traditional graphite structural configurations such as flat graphite rod, graphite plate, and graphite disk that have been commonly used as negative electrodes in MFCs are often applied as anodes in BPV systems.[101] Graphite, with its affordable cost, higher electron delocalization nature and low impurity content, offers a relatively high mechanical strength than carbon paper under extreme operational conditions. Although it does not have a high surface area, the relatively well characterized compact structure and reproducible smooth surface facilitate the quantitative measurement of biomass per unit area for fundamental electrochemical studies.[102,103] A dual chamber MFC that used a plain graphite plate as the anode acquired peak power densities of 41.5 ± 1.2 mW m^{-2} and 30.2 ± 0.8 mW m^{-2} using two photosynthetic microorganisms, namely *Synechococcus* sp. and *Chlorococcum* sp., while treating kitchen wastewater.[104] Moreover, the biofilm growth of *Chlamydomonas reinhardtii* on graphite rods in a photo microbial fuel cell (PMFC) was assessed in a series of studies with power densities of 0.009 mW m^{-2}, 0.82 mW m^{-2}, and 12.947 mW m^{-2}.[105–107] However, there are still several limitations of the graphite anode. Although the surface of the graphite anode appears to be rough under scanning microscopic examination (10 μm), it is nearly flat in comparison to the scale of photosynthetic

microbes (approximately 1 μm).[78] The graphite surface's brittle nature needs further improvement for scaling up practical devices.[56] Also, the low porosity and the presence of volatile compounds on the graphite surface will hinder the adhesion of microbial cells, resulting in low power density of BPV systems.[108] Therefore, to overcome these shortcomings, surface properties are altered by reshaping graphite into more three-dimensional materials such as graphite felt. Graphite felt (GF) has several unique characteristics such as loose texture, porous structure, compressibility, mechanical flexibility, and reasonable cost, which offers more space for bacterial growth.[109] Compared to other carbon-based materials (graphite sheet and carbon cloth), GF displays better performance as an electrode given its additive advantages of the extensive volumetric area.[109] The application of GF as the anode in BPV systems offers a vast volumetric area, considerable reduction in stack size containing various cells and increase in mass transport, which help maintain high current density.[110]

The performance of a graphite felt anode in a single chamber microbial solar cell (MSC) for the attachment of a self-organized photosynthetic biofilm was evaluated.[111] A photocurrent density of up to 86 mm^{-2} was reported on the 10th day under the constant illumination of 30 W m^{-2} with GF, which provided a large accessible surface area for the colonization of the microbial community and a uniform macroporous scaffolding for effective mass flow of the nutrients. In a follow-up study, the same research group examined the metabolism and interactions of two defined co-cultures of *Geobacter sulfurreducens* and *Chlamydomonas reinhardtii* using a graphite felt anode in a similar configuration.[112] The syntrophic association between the co-cultures yields a maximum current density of 120 mA m^{-2}, which is 0.3 times larger than that of another reactor with a hot spring inoculum. The carbon dioxide sequestration and bioenergy generation of *C. vulgaris* on a carbon felt surface were examined in a bubbling type photosynthetic algal microbial fuel cell. The maximum power density obtained was 1108.9 mW m^{-3}.[86] However, the electrochemical activity of commercial GF is generally low, limiting the power density and voltage efficiency of BPV systems.

Despite these favourable features exhibited by carbon, the carbonaceous anode's hydrophobic nature normally hinders the electron transfer efficiency. Hence, surface modifications are inevitable to enhance the carbon-based electrode's power performance in order to be used in electrochemical studies.[51] Moreover, the surface modification technique can also introduce different functional groups on the surface of carbon electrodes which promote biofilm formation.[113] Several studies

have illustrated that BPV systems configured with surface modified anodes exhibit better electrochemical performance, corrosion resistance and biocompatibility than those configured with unmodified anodes.[113,114] One of the most commonly employed surface modification approaches is using three-dimensional polymer templates to modify plane electrodes into promising bioanodes with increased surface area for better microbial cell adhesion in BPV systems with highly efficient performance.[113]

An upgrade to metallic electrodes is carbonaceous anodes that are relatively stiff with rougher surfaces for improved cell loading and adhesion per unit of surface area. Despite their frequent use in BESs, carbon electrodes have many limitations.[24] The hydrophobic nature of carbon materials usually requires physical or chemical surface modifications to facilitate bacterial attachment. Moreover, the electrical conductivity of carbon is three orders of magnitude lower than that of most metallic electrodes, *e.g.* the conductivity of copper is 5.8×10^7 S m^{-1} (ref. 67) whereas that of graphite is 3×10^4 S m^{-1}.[67] The specific electrical conductivity of these electrode materials can be compensated in a BES by increasing the electrode surface area, thus improving the capacitive performance of the electrode. Integrating a large size and surface area anode in a BPV system may be feasible for small, lab-based systems. In a scaled up industrial application, the high cost may completely collapse this electrochemical system's performance index. Most importantly, the dense black opaque nature of carbon electrodes limits the penetration of light to the photosynthetic biofilm, raising a major concern regarding their feasibility in BPV systems.

3.3. Transparent conducting oxide anodes

Transparent conducting oxide (TCO) anodes refer to inorganic semiconductor (indium, tin, zinc, or cadmium oxides, for example) films sputtered by vacuum deposition techniques to simultaneously combine the high transmittance value at $T >$ 85% in the visible light spectrum with a low resistivity of $\rho < 1 \times 10^{-3}$ Ω cm. The other most relevant properties are high thermal and chemical stability, low contact resistance, mechanical properties, high stretchability and tunable work function.[115] Among various TCO materials, tin-doped indium oxide (ITO) and fluorine-doped tin oxide (FTO) have set the market standard for BPV systems due to their suitable values of transparency (90% at 550 nm) and sheet resistance (10–30 Ω sq^{-1}) (Table 3).[62]

Biofilm formation of selected algal strains on ITO coated glass anodes was investigated to determine the efficiency of

Table 3 Common optical and electrical values of the ITO film, adapted from ref. 115^a

Material	Magnitude of sheet resistance (Ω sq^{-1})	Transmittance (%)	Wavelength (nm)	Figure of merit Haacke (Ω^{-1})	Figure of merit Coleman (Ω^{-1})
ITO/glass	10	80	Visible range	1.1×10^{-2}	159.8
ITO/PET	50	80	Visible range	2.1×10^{-3}	32.0

^{a} ITO, indium tin oxide; PET, polyethylene terephthalate.

Table 4 Summary of translucent electrode materials used in biophotovoltaic (BPV) systems[a]

Anode material	Anode configuration	Anode dimensions	Photosynthetic species	Reactor setup (type, temperature, electrolyte, mediator)	Light intensity	Maximum power or current density
Indium tin oxide (ITO) coated polyethylene terephthalate (PET) (Bombelli et al., 2011)[44]	Flat	Dimensions of the anodic chamber: 40 mm × 2 mm × 2 mm, surface area: 0.8 cm^{-2}	Synechocystis sp. PCC 6803	Biophotovoltaic devices, 25 °C, BG-11 medium, 25–35 mM ferricyanide	12 h light (229.5 μmol photons per m^2 or 50 W m^{-2}) and 12 h dark cycle	0.696 mW m^{-2}
Indium tin oxide (ITO) coated polyethylene terephthalate (PET) (McCormick et al., 2011)[52]	Flat	50 × 50 mm, surface area: 12.56 cm^{-2}	Synechocystis sp. PCC 6803	Mediator-free bio-photovoltaic cell system, 22 ± 2 °C, BG-11 medium	White light (45.9 μmol photons per m^2 s or 10 W m^{-2})	0.114 mW m^{-2}
Indium tin oxide (ITO) coated polyethylene terephthalate (PET) (McCormick et al., 2011)[52]	Flat	50 × 50 mm, surface area: 12.56 cm^{-2}	Chlorella vulgaris	Mediator-free bio-photovoltaic cell system, 22 ± 2 °C, 3N: BBM + vitamins	White light (45.9 μmol photons per m^2 s or 10 W m^{-2})	0.45 mW m^{-2}
Indium tin oxide (ITO) coated polyethylene terephthalate (PET) (McCormick et al., 2011)[52]	Flat	50 × 50 mm, surface area: 12.56 cm^{-2}	Dunaliella tertiolecta	Mediator-free bio-photovoltaic cell system, 22 ± 2 °C, mod F/2 + vitamins	White light (45.9 μmol photons per m^2 s or 10 W m^{-2})	7 mW m^{-2}
Indium tin oxide (ITO) coated polyethylene terephthalate (PET) (McCormick et al., 2011)[52]	Flat	50 × 50 mm, surface area: 12.56 cm^{-2}	Synechococcus sp. WH 5701	Mediator-free bio-photovoltaic cell system, 22 ± 2 °C, BG-11 medium	White light (45.9 μmol photons per m^2 s or 10 W m^{-2})	10 mW m^{-2}
Fluorine doped tin oxide (FTO) coated ceramic (Thorne et al., 2011)[62]	Porous	15 × 15 × 7.5 mm	Chlorella vulgaris	Photo-microbial fuel cells, Bold basal medium with 3-fold nitrogen and vitamin, 2.5 mM ferricyanide	Low monochromatic light illumination (55.08 μmol photons per m^2 s or 12 W m^{-2}) at 652 nm	14 mW m^{-2}
Fluorine doped tin oxide (FTO) coated glass (Thorne et al., 2011)[62]	Flat	15 × 15 × 7.5 mm	Chlorella vulgaris	Photo-microbial fuel cells, Bold basal medium with 3-fold nitrogen and vitamin, 2.5 mM ferricyanide	Low monochromatic light illumination (55.08 μmol photons per m^2 s or 12 W m^{-2}) at 652 nm	24 mW m^{-2}
Indium tin oxide (ITO) coated polyethylene terephthalate (PET) (Bombelli et al., 2012)[50]	Flat	100 × 20 mm^{-2}, surface area: 20 cm^{-2}	Pseudanabaena limnetica	Multi-channel mediator-free biophotovoltaic system with open air cathode, 22 ± 2 °C, BG-11 medium	2 h light (36.72 μmol photons per m^2 s or 8 W m^{-2}) and 2 h dark cycle	23.6 mW m^{-2}
Indium tin oxide (ITO) coated glass slide (Inglesby et al., 2013)[119]	Flat	20 × 20 × 1 mm	Arthrospira maxima	Photosynthetic microbial fuel cell, 25–35 °C, nutrient media with metal solution	91.8 μmol photons per m^2 s or 20 W m^{-2}	0.0248 mW m^{-2}
Indium tin oxide (ITO) coated polyethylene terephthalate (PET) (Bradley et al., 2013)[17]	Flat	Surface area: 12.56 cm^{-2}, working volume: 31.5 mL	Synechocystis sp. PCC 6803	Biological photo-voltaic systems, 21 ± 1 °C, BG-11 minimal medium with 5 mM NaHCO$_3$, 1 mM ferricyanide	5 W LED light at 40 μmol photons per m^2 s	0.039 ± 0.008 mW m^{-2}
Indium tin oxide (ITO) coated glass (Ng et al., 2014a)[19]	Flat	35 × 35 mm	Chlorella vulgaris (UMACC 051)	Single chamber biophotovoltaic device, 25 °C, Bold's basal medium	30 μmol photons per m^2 s	0.112 mW m^{-2}
Indium tin oxide (ITO) coated glass (Ng et al., 2014a)[19]	Flat	35 × 35 mm	Chlorella sp. (UMACC 313)	Single chamber biophotovoltaic device, 25 °C, Bold's basal medium	30 μmol photons per m^2 s	0.124 mW m^{-2}
Indium tin oxide (ITO) coated glass (Ng et al., 2014a)[19]	Flat	35 × 35 mm	Synechococcus elongatus (UMACC 105)	Single chamber biophotovoltaic device, 25 °C, Kosaric medium	30 μmol photons per m^2 s	0.313 mW m^{-2}

Table 4 (Contd.)

Anode material	Anode configuration	Anode dimensions	Photosynthetic species	Reactor setup (type, temperature, electrolyte, mediator)	Light intensity	Maximum power or current density
Indium tin oxide (ITO) coated glass (Ng et al., 2014a)[19]	Flat	35 × 35 mm	Spirulina platensis (UMACC 159)	Single chamber biophotovoltaic device, 25 °C, Kosaric medium	30 μmol photons per m² s	0.121 mW m⁻²
Indium tin oxide (ITO) on fluorine doped tin oxide (FTO) coated glass (Ng et al., 2014b)[116]	Flat	3.5 cm × 3.5 cm	Chlorella sp. (UMACC 313)	Biophotovoltaic system, 24 °C, Bold's basal medium	White fluorescent lamps (30 μmol photons per m² s) on a 12 : 12 hour light–dark cycle	0.13 mW m⁻²
Reduced graphene oxide coated glass (Ng et al., 2014b)[116]	Flat	3.5 cm × 3.5 cm	Chlorella sp. (UMACC 313)	Biophotovoltaic system, 24 °C, Bold's basal medium	White fluorescent lamps (30 μmol photons per m² s) on a 12 : 12 hour light–dark cycle	0.27 mW m⁻²
Nano porous indium tin oxide (ITO) on fluorine doped tin oxide (FTO) coated glass (Wenzel et al., 2018)[18]	Porous	1 cm⁻²	Synechocystis sp. PCC 6803	3D printed biophotovoltaic device, 30 °C, BG-11 medium + 10 mM PBS	LED white light, photon flux densities of ca. 500 μmol photons per m² s	3.77 mW m⁻²
Micro porous indium tin oxide (ITO) on fluorine doped tin oxide (FTO) coated glass (Wenzel et al., 2018)[18]	Porous	1 cm⁻²	Synechocystis sp. PCC 6803	3D printed biophotovoltaic device, 30 °C, BG-11 medium + 10 mM PBS	LED white light, photon flux densities of ca. 500 μmol photons per m² s	4.37 mW m⁻²
Nonporous indium tin oxide (ITO) coated polyethylene terephthalate (PET) (Wenzel et al., 2018)[18]	Porous	1 cm⁻²	Synechocystis sp. PCC 6803	3D printed biophotovoltaic device, 30 °C, BG-11 medium + 10 mM PBS	LED white light, photon flux densities of ca. 500 μmol photons per m² s	0.01 mW m⁻²
Nano porous indium tin oxide (ITO) on fluorine doped tin oxide (FTO) coated glass (Wenzel et al., 2018)[18]	Porous	1 cm⁻²	Nostoc punctiforme	3D printed biophotovoltaic device, 30 °C, BG-11 medium + 10 mM PBS	LED white light, photon flux densities of ca. 500 μmol photons per m² s	3.57 mW m⁻²
Nonporous indium tin oxide (ITO) coated polyethylene terephthalate (PET) (Wenzel et al., 2018)[18]	Porous	1 cm⁻²	Nostoc punctiforme	3D printed biophotovoltaic device, 30 °C, BG-11 medium + 10 mM PBS	LED white light, photon flux densities of ca. 500 μmol photons per m² s	0.04 mW m⁻²
Inverse opal indium tin oxide on fluorine doped tin oxide (FTO) coated glass (Zhang et al. 2018)[21]	Porous	Geometrical surface area: 0.75 cm⁻²	Synechocystis sp. PCC 6803	Three-electrode setup, BG-11 medium, 25 °C	LED white light, photon flux densities of ca. 500 μmol photons per m² s	45.9 μmol photons per m² s or 1 mW cm⁻² (λ 685 nm)	0.63 mW m⁻²

[a] BG-11, blue green-11 medium; PBS, phosphate buffered saline; power density was calculated by normalizing the power output to the surface area of the anode; unit conversion for light intensity was performed according to the coefficient values of Plant Growth Chamber Handbook.[75]

algal biofilms for power generation in BPV systems (Table 4). Out of the sixteen algal strains, four outperformed with regard to power output when grown directly on the ITO surface.[19,116] However, for the same BPV system, changing the anode material from ITO coated glass to reduced graphene oxide coated glass caused a 119% increased efficiency from green algae biofilm.[19]

The recent progress in physical vapour deposition methods of using TCO precursors allows the production of hierarchically structured electrode films with nano-roughness.[117] Glass or ceramic porous electrodes coated with ITO or FTO increase the available surface area to facilitate dense cell loading and biofilm interactions.[50] These highly porous structures were inspired by bones with pores and channel sizes specifically designed to accommodate the dimensions of *Synechocystis* sp. and to ensure light transmission, while overcoming the limitations of nutrient diffusion and mass transport across the biofilm.[21,118] For cyanobacteria, FTO anodes outperformed the benchmark carbon-based electrodes in terms of photocurrent density output of BPV systems.[62] A 16-fold increase in power density was observed when comparing carbon anodes coated with FTO *versus* carbon anodes.[62] In another study, a porous microcrystalline titanium dioxide substrate was coated with a layer of FTO through chemical vapour deposition to improve electrical conductivity. The authors attributed this higher performance to the porous electrode's surface chemistry that anchored the extensive extracellular matrix of *Chlorella vulgaris*.[62]

Another study monitored the *in situ* fluorescence and electrochemical performance of a filamentous cyanobacterium, *Arthrospira maxima*, on an ITO coated glass anode, although the system experienced low current density due to the low pH conditions produced by the cyanobacteria in the micro-environment between the cells and the anode, which degraded the ITO.[119] ITO-coated polyethylene terephthalate (ITO-PET), in the form of a flat electrode, demonstrated a high biofilm growth rate and power output for various photosynthetic species in BPV systems.[18,52] The performances of three different surface porosities of ITO coated anodes on the nano-metre and micrometre length scales were compared when using *Synechocystis* sp. PCC6803. A 300-fold increase in the current output was observed with both porous electrode types.[18]

The functionalization of an ITO electrode with PET as a coating agent was also investigated with photosynthetic biofilms grown from freshwater or marine species.[52] *Synechococcus* showed the highest power density (10 mW m^{-2}) and biofilm density on the ITO-PET electrode compared to the other three cultures.[52] Similarly, another study compared the performance of *Pseudanabaena limnetica* biofilms using different anode materials: ITO-PET, carbon paper, stainless steel, and polyaniline coated glass in a multi-channel mediator-free BPV system. The photosynthetic biofilm grown on ITO and stainless steel demonstrated the maximum power output and photoresponse whereas carbon paper was unsuitable for operation. Analysis of the effects of substrate surface energies and other surface characteristics such as roughness, hydrophobicity, CQ ratio and electron donor or acceptor capacity on cyanobacterial biofilms suggested a remarkable difference in cell adhesion, structure,

and extracellular matrix production on carbon paper compared to other materials.[50] The authors concluded that the material surface energy is a major factor determining BPV system performance without any consistent dependency on surface roughness.

In BPV systems, ITO or FTO doped glass electrodes significantly outperform carbon-based material power generation with a maximum reported power density of 24 mW m^{-2} compared to the 14 mW m^{-2} for carbon cloth.[62] However, the major drawbacks of TCOs must be considered, which include the production cost of base materials, feasibility of fabrication processes, and scalability for industry.[115] The demand of ITO in the touch panel market is increasing rapidly (around 35% annually) due to its use as an electrode in LEDs, LCDs, or transparent films and touch sensors in tablets, smartphones, or car devices.[120] ITO has several shortcomings in terms of market issues and the material's performance limitations.[121] One of the most significant challenges is that indium, necessary to achieve suitable conductivity, is a rare element on Earth, limiting long-term economic and ecological sustainability. Considering the dramatic rise in indium demand, this scarce resource is expected to deplete within a few decades.[122] The other major challenge is that biofilms developed on planar FTO glass electrodes were more prone to damage or removal from high shear flow than porous ceramic structures, indicating the significance of nanoscale surface roughness.[62] The cost and fragility of indium are strong arguments for exploring alternative transparent electrode materials. Therefore, over 50 companies around the world of different sizes are currently focusing their efforts toward the replacement of ITO transparent films.[115] It is expected that the alternatives to ITO will reach a combined market value of about $0.43 billion in 2025.[121] The launch of novel electrically conductive transparent materials and the development of new fabrication strategies to adapt these materials into different electrode architectures that enable rapid BPV system start-up will be of immense benefit to the field.

3.4. Polymer composite anodes

Conducting polymers particularly polypyrrole (Py), polyaniline (PANI) and poly(3,4-ethylenedioxythiophene):polystyrene sulfonate (PEDOT:PSS) have attracted considerable attention as anode doping materials owing to their electrical conductivity and environmental durability.[115] The polymer doped in the form of composites is expected to improve the anodic performance further. For example, nanocomposites of poly(3,4-ethylene dioxythiophene):polystyrene sulfonate (PEDOT:PSS) or graphite/polytetrafluoroethylene (PTFE) on carbon cloth were reported by Liu and his colleagues.[94] PTFE nanocomposites modified the graphite rods to produce a high performance bioanode for BPV systems. The graphite/PTFE nanocomposite significantly increased the microbial adhesion and electron transfer efficiency by creating nanostructures on the anodic surface (Table 5).[94] Similarly, combining the advantages of PEDOT:PSS and carbon cloth yields a maximum power density of 43.8 μW cm^{-2}, which is 27-fold higher than that of

Table 5 Application of polymer-modified anodes in biophotovoltaic (BPV) systems[a]

Anode material	Anode configuration	Anode dimensions	Photosynthetic species	Reactor setup (type, temperature, electrolyte, mediator)	Light intensity	Maximum power or current density
Osmium redox polymer-modified graphite rods (Hasan et al., 2014)[114]	Flat	Graphite rod diameter: 3.05 mm	Leptolyngbya sp. (CYN82)	Photo microbial fuel cell, 1 mM ferricyanide	Fibre optic light source with a light intensity of 2019.6 μmol photons per m^2 s or 440 W m^{-2}	481.5 mW m^{-2}
Osmium redox polymer-modified graphite rods (Hasan et al., 2017)[124]	Flat	Modified electrode active surface area: 0.0731 cm^{-2}, graphite rod diameter: 3.05 mm	Filamentous cyanobacteria	Photo microbial fuel cell, PBS buffer (10 mM phosphate buffer at pH 7.0 including 10 mM NaCl and 5 mM MgCl$_2$)	A light intensity of 40 mW cm^{-2} ($\approx$2000 μmol photons per m^2 s)	47.2 μA cm^{-2}
Carbon cloth modified with poly(3,4-ethylene dioxythiophene):polystyrene sulfonate (PEDOT:PSS) (Liu et al., 2017)[108]	Flat	0.07 cm^{-2}, 140 mL-sized anode chamber	Synechocystis sp. PCC 6803	Dual chamber miniaturized biological solar cell with an air cathode, 30 ± 2 °C, BG-11 medium	24 h light cycle (12 h light/dark)	438 mW m^{-2}
Carbon cloth modified with graphite/polytetrafluoroethylene (PTFE) composite (Liu et al., 2017)[108]	Flat	Projected surface area: 0.07 cm^{-2}, 140 mL-sized anode chamber	Synechocystis sp. PCC 6803	Dual chamber miniaturized biological solar cell with an air cathode, 30 ± 2 °C, BG-11 medium	24 h light cycle (12 h light/dark)	175 mW m^{-2}

[a] BG-11, blue green-11 medium; PBS, phosphate buffered saline; NaCl, sodium chloride; MgCl$_2$, magnesium chloride; power density was calculated by normalizing the power output to the surface area of the anode; unit conversion for light intensity was performed according to the coefficient values of *Plant Growth Chamber Handbook*.[75]

a microfluidic biological solar cell with a standard carbon cloth anode (1.6 μW cm^{-2}).[94]

In a series of studies,[114] different structures and redox potentials of osmium (Os) polymers were introduced as surface modification on a graphite anode to maximize the surface area and minimize the energy gap of photosynthetic cells with electrodes. In Os-polymer modified electrodes, the cationic Os-polymer acts as a surface adsorbed polymeric mediator. A strong electrostatic interaction with the anionic *P. pseudovolvox* cell membrane was formulated to improve the electrochemical communication by freely interacting with the photosynthetic reaction centre. Compared to traditional laborious annealing processes using a furnace, the spreading of the Os layer for surface modification is a clean and nontoxic process favouring direct electron transfer.[123,124]

The polymer is a promising surface modification material owing to its hydrophilicity,[125] stability,[126] and biocompatibility,[127] all of which is expected to improve the microbial density on the anode surface. Simultaneously, the carbon increased the electrocatalytic activities and mechanical properties.[128] However, the viscous polymer often blocks carbon cloth pores.[88,93] Thus, limiting the microbial attachment only on the outer surface hindered the effective mass diffusion of nutrients and halted the PBV device's performance in long-term operations.

4. Strategies to increase the surface area

The anode composition, structure design, and dimensions are crucial factors in determining the biofilm formation rate on the electrode surface and the development of electrical connections among immobilised cells. Moreover, the anode's surface charge density and physicochemical properties are well established as influencing factors of bacterial attachment. The surface functional groups of electrodes interfacing the biocatalytic machinery near the routes of electron transfer could interfere with the rate and mechanism of extracellular electron transfer at this interface.[53] The exact metabolic mechanisms involved in photosynthetic microorganism mediated photocurrent production remain unclear,[25] although many studies focused on optimising electrode materials for mediator-free systems to facilitate favourable conversion efficiency rate and power density. Researchers have tried to develop electrodes that enhance electrochemical communication between microbes, thus lowering potential losses in BPVs.[62,99,114] Due to the comparatively low power outputs, plain unmodified carbonaceous anodes with low porosity similar to the ones used in BES research for electrochemically active biofilms are somewhat scarce in whole cell based BPV systems. Therefore, the practices of surface treatments and structural modifications of the base material established from the literature on BESs have found their way into BPV systems to improve biofilm–electrode interaction. Some examples of the research to enhance electrode materials include the application of surface treatment *via* physical or chemical methods, electroactive coatings, and the use of composite electrodes.[50,129] Although these approaches enhanced BPV system performance for the current generation and scalability, the net output is yet considerably lower than what can be achieved through converting organic substrates to electricity in microbial fuel cells.[16]

4.1. Surface modifications

A relatively common approach to increase the conductivity and active surface area for microbial attachment is to modify the surface physical chemistry of electrodes by varying the number and nature of the functional groups present on the electrode surface. Several physical and chemical surface treatments have been effectively used to improve the biofilm formation and performance of BPV systems.[114,130] ITO electrodeposition,[131] soaking method,[132] sintering process,[133] chemical vapour deposition technique,[134] ammonia gas treatment,[135] and high-temperature carburisation[29] are just a few examples of modification methods. In order to improve the anode performance various artificial electron mediators such as 9,10-anthraquinone-2,6-disulfonate,[136] neutral red,[132] methylene blue[137] and Mn(IV)[132] have been immobilised on the anode surface to support electron transfer from the exoelectrogenic bacteria to the anode. These mediator incorporated anodes greatly enhanced the power density of their respective systems when compared with unmodified anodes as reported in previous studies. Similarly, thin layers of electroactive organic polymers (*e.g.* polypyrrole [PPy],[138] polyethyleneimine,[136] polyaniline [PANI])[130] deposited on the anode surface have also been reported to improve current generation. This increased power density using modified anodes in the same configuration and operating parameters as the bare form could be attributed to improved physicochemical properties, higher surface area and enhanced electrochemical communication between the bacterial cell and anode surface.[130] Due to the lack of quantitative data comparing the surface areas of modified and unmodified anodes in the literature, power density has been used as an indirect indicator in this review. The modified anode materials have rough surfaces with higher surface area which provides additional space for the colonization of bacterial population per unit area and gives increased bacteria or mediator access to the surface.[130] Moreover, the electrostatic attraction between positively charged polymers and negatively charged bacterial cells further increases adhesion and electron transfer.[138] For example, pretreatment of graphite rods with osmium redox polymers affects the electron transfer from immobilized cyanobacterial cells through different redox complexes. The presence of osmium redox centres in the polymer matrix appears to favor photo-electrochemical communication. However, these multistep modification approaches are time-consuming and require complex setups and extreme temperature conditions.[84] Moreover, neither sufficient data on the physical, chemical, and biological effects of these modifications on biofilm formation rates nor the nature of these surface treatments is precisely highlighted in these preliminary studies. The main challenges in improving the performance of BPV systems are the development of cost-effective materials and architectures that can

increase the space available for direct microbial attachment.[78] Thus, there lies an urgent need for more simple and effective techniques to improve electrode performance in BPV system studies.

4.2. Porosity

Another modification approach, which can be expected to provide sizeable accessible surface areas for bacteria and promote efficient bio-electron transfer, is increasing the surface roughness (*i.e.* increased holes, porosity, and/or steps) while using different materials for electrode fabrication.[62,101] New fabrication strategies such as polystyrene microsphere templating[18] and additive manufacturing[139] can adapt the structure of electrode materials into different architectures with desirable electrical conductivity, optical transparency, hydrophilic surface chemistry, and nano-scale surface roughness.[140] Compared to smooth or planar electrodes, a highly porous structure significantly improves the intercellular communication, oxygen influx and nutrient transport across the surrounding microbial cells and creates a beneficial microenvironment by removing metabolic wastes.[118] The before and after scanning electron microscopic (SEM) images of a polypyrrole coated reticulated vitreous carbon anode reveal a three-dimensional network of interconnected pores (microns) that offers an ideal microenvironment for bacteria to reside inside.[138] The hierarchically structured electrodes were originally designed considering the physical properties of isolated photosystems to allow light penetration which was later adapted for microbe attachment. The interconnecting channels of the porous material do not get clogged by biofilm growth, thus preventing the cells present in the electrode's interior from entering the nutrient starvation phase.[141,142] Another benefit of materials with pores is that they support healthy biofilm growth under strong shear flow conditions, which is a common problem in the operation of BPV systems.[51]

4.3. Additive manufacturing

Beyond surface roughness, a more promising and developing area is the production of complex three-dimensional (3D) structures specifically intended to improve cell number per unit surface area projected on the electrodes, called additive manufacturing.[139] An important benchmark of incorporating 3D anodes of complex geometries within BPV systems is provided by an elegant proof of concept study illustrating a novel solid wall electrode fabricated through a single photolithography step.[143] Combining the advantages of microsolidic approaches to explore the surface tension of low melting point alloys resulted in a self-aligned electrode within the microfluidic device's channels, which directly connected the metal electrodes with the electrolyte within the microfluidic channels.[143] Controlled single step photolithography has attracted significant interest owing to its ability to produce well-defined 3D electrodes with reproducible morphology and stable electronic properties for microfluidic BPV systems.[143] This is an underexplored engineering approach to fabricate anodes with higher geometric surface area for microbial attachment which

may expand the scope of BPV systems to other renewable energy generating bioelectrochemical systems.[139] In another study, a simple, environmentally friendly, cost-efficient and time saving soft-lithography approach was proposed to prepare a self-aligned electrode from InSnBi alloy, facilitating the physical proximity between the cells and electrode required for mediator-free operation.[45] The resultant electrode with miniaturised geometries allowed the favourable physical proximity of cells and significantly increased the power densities. A peak power density of 294 ± 17 mW m^{-2} was reported under illumination for a chlorophyll concentration of 100 μM,[45] which is 191% higher than that of a BPV system with a standard ITO anode.[50] The authors attributed this high performance to the biofilm's physical proximity to the anode, which was thought to lower the device's internal resistance. Moreover, the anodic chamber's microscopic setup created a large active surface to volume ratio, which improves reaction kinetics, mass transport, and cellular communication.[45]

The improvement in power output resulting from these modifications was attributed to more favourable microbial adhesion provided by the increased surface area.[49,62] However, a major drawback associated with the development of these surface and/or structural engineering approaches is the lack of information on the direct impact of these modifications on the electrode's electrochemical properties, biofilm formation, and attached cell biochemical viability. Studies on additive manufacturing of electrodes for BESs can provide some mechanistic insight into the impact of geometric structures.[78] In-depth investigation of modification approaches to effectively increase the wiring of microbial cells to the electrode surface *via* redox polymers and additive manufacturing should be conducted.[142] This represents a significant challenge as a defined pore size capable of specifically harbouring microbial population superior to that of planar electrodes has yet to be identified.[62]

The high cost and brittle properties of metal oxide coated glass hindered its practical application in a long-term BPV system.[115] Seeking an economically viable and highly catalytic alternative material to replace metal oxides is a hot issue for sustainable development.[125] Several anode candidates, including metallic,[68] carbonaceous,[90] alloy,[71] and conductive polymer-based materials,[94] have been widely examined in BPV systems but their power output is still lower than that in BESs. Increasing the anode surface area is an effective way to improve BPV system performance.[78] However, the increase of anode size in the conventional two-dimensional electrode configuration is accompanied by an increase in operational volume and infrastructure costs.[78] Inexpensive three-dimensional (3D) electrodes offer a solution to this problem, as they can support microbial attachment besides increasing power density, which theoretically should improve the performance of BPV systems.[139] To date, several challenges in terms of scale and production are associated with the use of three-dimensional electrodes in bioelectrochemical systems.[118] Moreover, the search for stable three-dimensional electrode materials and suitable manufacturing techniques is still ongoing, which needs to be sorted out before any future application.[78] The primary concern

is optimising the physical and chemical properties of novel anode materials to further improve their catalytic activity for high-performance BPV systems. Maybe a concerted effort focusing on innovative fabrication approaches along with novel electrically conductive opaque materials for anodes would be more beneficial in this field.

5.   Discussion

BPV systems are light dependent BESs that offer advantages of self-sustainability, self-repair and no processing requirements compared to abiotic photovoltaic cells.[25] The research in this field is still in its early stages of development primarily relying on the findings of microbial fuel cells for guidance in system setups. Despite the previous attempts to differentiate BPV systems from the rest of BESs,[16] how the current nomenclature and parameters ought to be applied in relevant studies is not systematically organized by fuel cell scientists. There are many classes of BESs, differing in electrochemical arrangement, fuel source, microbial ecology, and purpose; in turn, this complexity is met with a variety of synonymous terminologies. The use of terminologies such as photoMFC, biosolar panel, and microbial battery interchangeably with the BPV system in the literature increases categorical ranks' complexity. This exercised classification should be made obvious to avoid ambiguity and nomenclature must gain a wider acceptance among researchers.

Attempts to calculate the maximum achievable power densities for photoMFCs (3000 mW m^{-2})[144] and BPV systems (7700 mW m^{-2})[16] have been previously made under optimum laboratory conditions. However, estimation of the potential of BPV systems in real life natural settings such as temperature and light variations must be considered, along with the energy conversion efficiency of these systems. The power outputs reported for the BPV systems so far have failed to meet this theoretically estimated fraction, highlighting the need for targeted optimization of design, biological material, and light

heterogenicity for future applications outside the lab. Despite the numerous efforts to systematically optimize the performance of different components of BPV systems,[52] comparing the findings emerging from these studies remains challenging due to the differing conditions between studies and the differing methods used to measure and report both the conditions and the resulting cell behavior. As has been noted previously, data reporting within the literature would be well served by converting measurements of conditions, such as light quality and intensity distribution in relation to frequency, to standardized the reported results in terms of SI units used for power or current density, and whether the data present the voltage at peak or at steady states.[24] Details of electrode dimensions and surface areas used in experimental setups are necessary to interpret the reported data when considering differing cell designs, but these specifics are rarely available. The surface difference between naked and modified anodes when compared using SEM has revealed enhanced surface area with rough texture which is believed to provide favourable electroactive sites for the building of a better biofilm leading to higher kinetic activity and power generation than those of their unmodified counterparts confirmed *via* electrochemical techniques.[145] Hence, to draw a fair comparison of the reported power densities it is crucial to normalize reported data with regard to the independent variables (such as temperature, pH, light, electrolyte, electrode material, surface modifications and BPV system design) of each study.

An attempt to evaluate the performance efficiency of different BPV systems reported in previous studies was made (ESI Table S1†) by considering the value of peak power output (mW m^{-2}) against total light intensity (W m^{-2}) used in experiments (Fig. 5). These conversions have been performed based on established best-practice approximations from the literature.[75] Due to the lack of complete spectral data in the literature of a particular light source these approximations are the best possible conversions, as a rigorous conversion between number of photons and energy measurement based on spectral flux
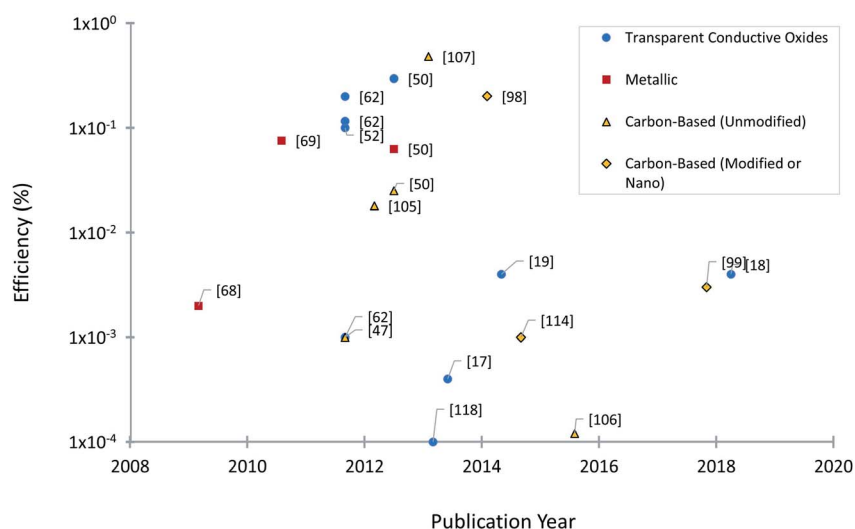

Fig. 5 The performance efficiency (%) of biophotovoltaic (BPV) systems reported in the past two decades.

distribution is not possible.[75] In the future, researchers should adopt the best practice of utilising the 1 Sun AM 1.5G reference spectrum, at a measured flux reported in mW m^{-2} units, for incident lighting, to allow comparison within the literature and to better represent the intended BPV use case of exploiting natural lighting.[146] The maximum performance efficiency was reported by Lan *et al.* (2013) achieving 0.4% with a dual chamber photo microbial fuel cell containing osmium polymer modified graphite rods.[107] However, due to the variations in cell design between the compared studies, it is difficult to say whether this high performance efficiency was a result of the anode's influence or better attributed to another specification of this design, such as catholyte composition ($K_3[Fe(CN)_6]$ + KH_2PO_4 + NaCl) or its 500 mL working volume, which is higher than those in the other studies being compared. Within the field of BPV systems, Bombelli *et al.* (2012) achieved 0.295% with a multichannel mediator-free BPV system with an ITO coated PET anode and an open-air cathode.[50] The favourable electrochemical interaction of photosynthetic microbes with the material characteristics of ITO coated PET (*e.g.* surface roughness, surface total energy, surface electron donor capacity and CQ ratio) could be an important factor determining the maximum performance.[50] However, the higher cathodic surface area exposed to volume ratio provided by five open chambers (20 mL) and proximity of both electrodes (5 mm apart) in the multichannel mediator-free BPV system with the open air cathode cannot be ignored. The next most efficient BPV system was reported by Thorne *et al.* achieving 0.2%, and utilizing a FTO coated glass anode,[62] a closely related material to that used by Bombelli *et al.* (2012).[50]

Additional studies in this normalized comparison would be ideal; however, the normalization methods employed limit our ability to analyse data from studies where particular design parameters were not reported; typically, these were not provided due to those studies reporting the effect of changing specific parameters within an otherwise static system design, and thus the other details were unnecessary to include beyond a summary of the system (ESI Table S2†). This limits the ability to reliably convert all available studies to a representative measure of performance efficiency for comparison without risk of misrepresentation. Thus, we suggest that BPV system research would benefit by establishing standard procedures for reporting power output and the input of light in terms of power intensity (W m^{-2}) and light flux density (W m^{-2}), both normalized to the cross-sectional area of the cell. Overall, the most effective materials are ITO coated PET and FTO coated glass with flat non-porous surfaces. Thus, further application of parametric design analysis and detailed design of electrodes with porous 3D design is an unexplored avenue with significant potential for success.

The influence of the biological material including photosynthetic components (whole cells or photosystems), composition of microbial community (mixed or pure culture), and microbial species (cyanobacterial or algal) on BPV system power output cannot be ignored. Different inoculum size, culture conditions (temperature, pH, and light intensity) and methods

used to initiate biofilm formation on the anode make it even more difficult to systematically compare previous studies.

Apart from the direct growth metrics such as total biomass (wet or dry) and cell count commonly used to measure the amount of anode inoculum in a BPV system, the cell loading of cyanobacteria can also be quantified indirectly *via* total chlorophyll content.[147] As turbidity and dry weight are indirect measures of biomass, quantifying both dead and living cells, chlorophyll content would be more suitable photosynthetic based systems. However, it must be noted here that even chlorophyll content is subject to variation with environmental conditions, mutations, stress response and from organism to organism.[147] The lack of standardized measure for the size of inoculum to be used in BPV system anodes is problematic,[24] and simply reporting the chlorophyll content of the biological material while ignoring different chlorophyll types and the ratio of these types may also be insufficient.[148] Quantifying the cell loading before and after BPV system experiments might help overcome the possible fluctuations in variables associated with the growth curve and biofilm sloughing, as advised elsewhere.[24] Standardization of BPV system design, data reporting, and ideal anode will make these findings relevant and helpful in laying a foundation for more advanced research in the fields of electron transfer, genetic modifications, and pilot-scale BPV solar panels.

6. Concluding remarks

The efficiency of contemporary BPV systems in transducing light energy to electricity is generally quite lower than that of other sunlight harvesting systems and experimental efforts are required to overcome the limitations of light delivery, stability of anodic culture and activation losses. Although the mechanics of BPV systems generally resembles that of microbial fuel cells, electric current is generated by illumination of anode associated oxygenic photosynthetic microorganisms. Hence, more commonly used optically opaque dark electrodes that obstruct light transmission are not suitable for power generation by BPV systems. In this review, we have addressed electrode materials and planar surface designs as the major performance limiting factors associated with BPV systems and the recent progress in structural modifications to improve the overall performance. In general, the prerequisites for ideal electrode materials are electrical conductivity, high surface area, chemical stability, low cost, and accessibility. As summarized here, different electrode configurations from flat metallic structures to three-dimensional transparent conducting oxides have been studied and exploited in BPV systems. Chemically inert metals such as stainless steel have emerged as promising low-cost anode materials for electricigens. However, research is in progress for alternative materials due to their inadequate surface roughness. Carbonaceous anodes are widely employed in BPV systems due to their high electrical conductivity, chemical stability, low cost, and biocompatibility. However, the illumination dependent metabolism of photosynthetic microorganisms makes their implementation unfeasible for BPV system applications. Even though transparent conductive oxides are the best reported

anodes so far, their integration on a commercial scale is limited because of their high cost and fragility. The suitability of cost-effective alternative materials for BPV system anodes has yet to be unequivocally examined. The overall analysis of the anode material's economic viability for BPVs is premature at present, due to the rapid improvement of material choice and designs. Future parametric studies on electrode materials and configurations in BPV systems will be a crucial tool for pursuing theoretical maximum power density.

Author contributions

Maira Anam: conceptualization, data curation, writing – original draft, writing – review & editing, visualization. Helena I. Gomes: writing – review & editing, supervision, funding acquisition. Geoffrey Rivers: writing – review & editing, supervision, visualization, conceptualization, funding acquisition. Rachel L. Gomes: writing – review & editing, supervision, funding acquisition. Ricky Wildman: writing – review & editing, supervision.

Conflict of interest

The authors declare no conflict of interest.

Acknowledgements

References

1 H. Ritchie and M. Roser, *Our World in Data 2020*, Published online at OurWorldInData.org, Retrieved from: https://ourworldindata.org/energy, Online resource.

2 IPCC, Summary for Policymakers, in *Global Warming of 1.5 °C. An IPCC Special Report on the impacts of global warming of 1.5°C above pre-industrial levels and related global greenhouse gas emission pathways, in the context of strengthening the global response to the threat of climate change, sustainable development, and efforts to eradicate poverty*, World Meteorological Organization, Geneva, Switzerland, 2018, p. 32, https://www.ipcc.ch/sr15/chapter/spm/.

3 J. J. Olmos and J. Kargul, *Acta Soc. Bot. Pol.*, 2014, **83**, 423–440.

4 A. Larkum, *Harvesting solar energy through natural or artificial photosynthesis: Scientific, social, political and economic implications*, 2011, vol. 2012, pp. 1–19.

5 IEA, 2012.

6 T. Blaschke, M. Biberacher, S. Gadocha and I. Schardinger, *Biomass Bioenergy*, 2013, **55**, 3–16.

7 D. Das, Introduction, in *Microbial Fuel Cell*, ed. D. Das, 2018.

8 E. Kabir, P. Kumar, S. Kumar, A. A. Adelodun and K.-H. Kim, *Renewable Sustainable Energy Rev.*, 2018, **82**, 894–900.

9 R. E. Blankenship, D. M. Tiede, J. Barber, G. W. Brudvig, G. Fleming, M. Ghirardi, M. R. Gunner, W. Junge, D. M. Kramer, A. Melis, T. A. Moore, C. C. Moser, D. G. Nocera, A. J. Nozik, D. R. Ort, W. W. Parson, R. C. Prince and R. T. Sayre, *Science*, 2011, **332**, 805.

10 Energysage, 2020.

11 J.-K. Choi and V. Fthenakis, *Environ. Sci. Technol.*, 2010, **44**, 8678–8683.

12 C. M. Motta, R. Cerciello, S. De Bonis, V. Mazzella, P. Cirino, R. Panzuto, M. Ciaravolo, P. Simoniello, M. Toscanesi, M. Trifuoggi and B. Avallone, *Environ. Pollut.*, 2016, **216**, 786–792.

13 W. Chen, J. Hong, X. Yuan and J. Liu, *J. Cleaner Prod.*, 2016, **112**, 1025–1032.

14 I. Lillo-Bravo, P. González-Martínez, M. Larrañeta and J. Guasumba-Codena, *Energies*, 2018, **11**, 363.

15 N. Sekar and R. Ramasamy, *Electrochem. Soc. Interface*, 2015, **24**, 67–73.

16 A. J. McCormick, P. Bombelli, R. W. Bradley, R. Thorne, T. Wenzel and C. J. Howe, *Energy Environ. Sci.*, 2015, **8**, 1092–1109.

17 R. W. Bradley, P. Bombelli, D. J. Lea-Smith and C. J. Howe, *Phys. Chem. Chem. Phys.*, 2013, **15**, 13611–13618.

18 T. Wenzel, D. Härtter, P. Bombelli, C. J. Howe and U. Steiner, *Nat. Commun.*, 2018, **9**, 1–9.

19 F.-L. Ng, M. M. Jaafar, S.-M. Phang, Z. Chan, N. A. Salleh, S. Z. Azmi, *et al.*, *Sci. Rep.*, 2014, **4**, 7562.

20 O. Yehezkeli, R. Tel-Vered, J. Wasserman, A. Trifonov, D. Michaeli, R. Nechushtai and I. Willner, *Nat. Commun.*, 2012, **3**, 1–7.

21 J. Z. Zhang, P. Bombelli, K. P. Sokol, A. Fantuzzi, A. W. Rutherford, C. J. Howe and E. Reisner, *J. Am. Chem. Soc.*, 2018, **140**, 6–9.

22 J. Calkins, Y. Umasankar, H. O'Neill and R. Ramasamy, *Energy Environ. Sci.*, 2013, **6**, 1891–1900.

23 R. I. Pinhassi, D. Kallmann, G. Saper, H. Dotan, A. Linkov, A. Kay, V. Liveanu, G. Schuster, N. Adir and A. Rothschild, *Nat. Commun.*, 2016, **7**, 12552.

24 L. T. Wey, P. Bombelli, X. Chen, J. M. Lawrence, C. M. Rabideau, S. J. L. Rowden, J. Z. Zhang and C. J. Howe, *ChemElectroChem*, 2019, **6**, 5375–5386.

25 J. Tschörtner, B. Lai and J. O. Krömer, *Front. Microbiol.*, 2019, **10**, 866.

26 M. Rosenbaum and U. Schröder, *Electroanalysis*, 2010, **22**, 844–855.

27 N. Schuergers, C. Werlang, C. M. Ajo-Franklin and A. A. Boghossian, *Energy Environ. Sci.*, 2017, **10**, 1102–1115.

28 G. Saper, D. Kallmann, F. Conzuelo, F. Zhao, T. N. Tóth, V. Liveanu, S. Meir, J. Szymanski, A. Aharoni and W. Schuhmann, *Nat. Commun.*, 2018, **9**, 1–9.

29 M. Rosenbaum, F. Zhao, M. Quaas, H. Wulff, U. Schröder and F. Scholz, *Appl. Catal., B*, 2007, **74**, 261–269.

30 Z. He, J. Kan, F. Mansfeld, L. T. Angenent and K. H. Nealson, *Environ. Sci. Technol.*, 2009, **43**, 1648–1654.

31 S. Liu, H. Song, X. Li and F. Yang, *Int. J. Photoenergy*, 2013, **2013**, 172010.

32 V. Vohra, *Materials*, 2018, **11**, 2579.

33 D. Wang, W. Wei and Y. H. Hu, *Ind. Eng. Chem. Res.*, 2020, **59**, 10457–10463.

34 N. Al-Dahoudi, A. Alkahlout, H. Saleh, N. Al-Dahoudi, T. El-Agez, S. Taya and M. Abdel-latif, *Turk. J. Phys.*, 2015, **1**(3), 272–279.

35 A. A. Bakulin, A. Rao, V. G. Pavelyev, P. H. van Loosdrecht, M. S. Pshenichnikov, D. Niedzialek, J. Cornil, D. Beljonne and R. H. Friend, *Science*, 2012, **335**, 1340–1344.

36 M. Grätzel, *Nature*, 2001, **414**, 338–344.

37 X. Xiao, H.-q. Xia, R. Wu, L. Bai, L. Yan, E. Magner, S. Cosnier, E. Lojou, Z. Zhu and A. Liu, *Chem. Rev.*, 2019, **119**, 9509–9558.

38 G. Squadrito and P. Cristiani, *Microbial and enzymatic fuel cells*, 2016, pp. 147–173.

39 J.-H. Tian, R. Lacroix, E. Desmond-Le Quéméner, C. Bureau, C. Midoux and T. Bouchez, *bioRxiv*, 2019, 609909.

40 M. Ramírez-Moreno, P. Rodenas, M. Aliaguilla, P. Bosch-Jimenez, E. Borràs, P. Zamora, V. Monsalvo, F. Rogalla, J. M. Ortiz and A. Esteve-Núñez, *Front. Energy Res.*, 2019, **7**, 135.

41 O. Bretschger, A. Obraztsova, C. A. Sturm, I. S. Chang, Y. A. Gorby, S. B. Reed, D. E. Culley, C. L. Reardon, S. Barua and M. F. Romine, *Appl. Environ. Microbiol.*, 2007, **73**, 7003–7012.

42 D. R. Lovley and D. J. F. Walker, *Front. Microbiol.*, 2019, **10**, 2078.

43 C. Leang, X. Qian, T. Mester and D. R. Lovley, *Appl. Environ. Microbiol.*, 2010, **76**, 4080–4084.

44 P. Bombelli, R. W. Bradley, A. M. Scott, A. J. Philips, A. J. McCormick, S. M. Cruz, A. Anderson, K. Yunus, D. S. Bendall, P. J. Cameron, J. M. Davies, A. G. Smith, C. J. Howe and A. C. Fisher, *Energy Environ. Sci.*, 2011, **4**, 4690–4698.

45 P. Bombelli, T. Müller, T. W. Herling, C. J. Howe and T. P. Knowles, *Adv. Energy Mater.*, 2015, **5**, 1401299.

46 H. Zhu, H. Meng, W. Zhang, H. Gao, J. Zhou, Y. Zhang and Y. Li, *Nat. Commun.*, 2019, **10**, 4282.

47 P. Bombelli, R. W. Bradley, A. M. Scott, A. J. Philips, A. J. McCormick, S. M. Cruz, A. Anderson, K. Yunus, D. S. Bendall and P. J. Cameron, *Energy Environ. Sci.*, 2011, **4**, 4690–4698.

48 S. Gadkari, S. Gu and J. Sadhukhan, *Chem. Eng. J.*, 2018, **343**, 303–316.

49 N. Mano, *Curr. Opin. Electrochem.*, 2020, **19**, 8–13.

50 P. Bombelli, M. Zarrouati, R. J. Thorne, K. Schneider, S. J. Rowden, A. Ali, K. Yunus, P. J. Cameron, A. C. Fisher and D. I. Wilson, *Phys. Chem. Chem. Phys.*, 2012, **14**, 12221–12229.

51 K. Schneider, R. J. Thorne and P. J. Cameron, *Philos. Trans. R. Soc., A*, 2016, **374**, 20150080.

52 A. J. McCormick, P. Bombelli, A. M. Scott, A. J. Philips, A. G. Smith, A. C. Fisher and C. J. Howe, *Energy Environ. Sci.*, 2011, **4**, 4699–4709.

53 A. Kumar, L. H.-H. Hsu, P. Kavanagh, F. Barrière, P. N. L. Lens, L. Lapinsonnière, J. H. Lienhard V, U. Schröder, X. Jiang and D. Leech, *Nat. Rev. Chem.*, 2017, **1**, 0024.

54 D. Natarajan and T. Van Nguyen, *J. Power Sources*, 2004, **135**, 95–109.

55 Mustakeem, *Mater. Renew. Sustain. Energ.*, 2015, **4**, 22.

56 S. Srikanth, T. Pavani, P. N. Sarma and S. Venkata Mohan, *Int. J. Hydrogen Energy*, 2011, **36**, 2271–2280.

57 T. Yamashita and H. Yokoyama, *Biotechnol. Biofuels*, 2018, **11**, 39.

58 E. Taşkan, S. Bulak, B. Taşkan, M. Şaşmaz, S. El Abed and A. Elabed, *Bioelectrochemistry*, 2019, **128**, 118–125.

59 J. Kramer, S. Soukiazian, S. Mahoney and J. Hicks-Garner, *J. Power Sources*, 2012, **210**, 122–128.

60 H.-Y. Wang, A. Bernarda, C.-Y. Huang, D.-J. Lee and J.-S. Chang, *Bioresour. Technol.*, 2011, **102**, 235–243.

61 A. Choudhury, L. Barbora, D. Arya, B. Lal, S. Subudhi, S. V. Mohan, S. Z. Ahammad and A. Verma, *Eng. Life Sci.*, 2017, **17**, 186–192.

62 R. Thorne, H. Hu, K. Schneider, P. Bombelli, A. Fisher, L. M. Peter, A. Dent and P. J. Cameron, *J. Mater. Chem.*, 2011, **21**, 18055–18060.

63 J. Li, J. Hu, C. Yang, W. Pu, H. Hou, J. Xu, B. Liu and J. Yang, *RSC Adv.*, 2019, **9**, 8700–8706.

64 P. C. Hallenbeck, *Microbial technologies in advanced biofuels production*, Springer, 2012.

65 D. Recio-Garrido, M. Perrier and B. Tartakovsky, *Chem. Eng. J.*, 2016, **289**, 180–190.

66 H. Wang and Z. J. Ren, *Biotechnol. Adv.*, 2013, **31**, 1796–1807.

67 A. Baudler, I. Schmidt, M. Langner, A. Greiner and U. Schröder, *Energy Environ. Sci.*, 2015, **8**, 2048–2055.

68 C.-C. Fu, C.-H. Su, T.-C. Hung, C.-H. Hsieh, D. Suryani and W.-T. Wu, *Bioresour. Technol.*, 2009, **100**, 4183–4186.

69 C.-C. Fu, T.-C. Hung, W.-T. Wu, T.-C. Wen and C.-H. Su, *Biochem. Eng. J.*, 2010, **52**, 175–180.

70 C.-C. Lin, C.-H. Wei, C.-I. Chen, C.-J. Shieh and Y.-C. Liu, *Bioresour. Technol.*, 2013, **135**, 640–643.

71 P. Kaibo, J.-R. Bai, Q.-Y. Chen and Y.-H. Wang, *Modified Stainless Steel as Anode Materials in Bioelectrochemical Systems*, 2020, pp. 165-184.

72 S. F. Ketep, A. Bergel, A. Calmet and B. Erable, *Energy Environ. Sci.*, 2014, **7**, 1633–1637.

73 E. Bazdar, R. Roshandel, S. Yaghmaei and M. M. Mardanpour, *Bioresour. Technol.*, 2018, **261**, 350–360.

74 Y. Liang, H. Feng, D. Shen, Y. Long, N. Li, Y. Zhou, X. Ying, Y. Gu and Y. Wang, *J. Power Sources*, 2016, **324**, 26–32.

75 R. W. Langhans and T. Tibbitts, *Plant growth chamber handbook*, 1997.

76 P. Zhang, D. Xu, Y. Li, K. Yang and T. Gu, *Bioelectrochemistry*, 2015, **101**, 14–21.

77 F.-l. Xu, J.-z. Duan, C.-g. Lin and B.-r. Hou, *J. Iron Steel Res. Int.*, 2015, **22**, 715–720.

78 X. Xie, C. Criddle and Y. Cui, *Energy Environ. Sci.*, 2015, **8**, 3418–3441.

79 N. Abdu, A. A. Abdullahi and A. Abdulkadir, *Environ. Chem. Lett.*, 2017, **15**, 65–84.

80 W. Zhang, S. Zhu, R. Luque, S. Han, L. Hu and G. Xu, *Chem. Soc. Rev.*, 2016, **45**, 715–752.

81 R. C. Alkire, P. N. Bartlett and J. Lipkowski, *Electrochemistry of carbon electrodes*, John Wiley & Sons, 2015.

82 R. Sekar, V. Venugopalan, K. Satpathy, K. Nair and V. Rao, in *Asian Pacific Phycology in the 21st Century: Prospects and Challenges*, Springer, 2004, pp. 109–116.

83 J. Cao, W. Yuan, Z. Pei, T. Davis, Y. Cui and M. Beltran, *J. Manuf. Sci. Eng.*, 2009, **131**(6), 645051–645054.

84 M. Zhou, M. Chi, J. Luo, H. He and T. Jin, *J. Power Sources*, 2011, **196**, 4427–4435.

85 C.-T. Wang, Y.-S. Huang, T. Sangeetha, Y.-M. Chen, W.-T. Chong, H.-C. Ong, F. Zhao and W.-M. Yan, *Bioresour. Technol.*, 2018, **255**, 83–87.

86 M. Li, M. Zhou, J. Luo, C. Tan, X. Tian, P. Su and T. Gu, *Bioresour. Technol.*, 2019, **280**, 95–103.

87 R. Jain, D. Tiwari, S. Sharma and P. Mishra, *J. Sci. Ind. Res.*, 2015, **74**, 308–314.

88 R. Mohammadzadeh Kakhki, *Arabian J. Chem.*, 2019, **12**, 1783–1794.

89 K. S. Madiraju, D. Lyew, R. Kok and V. Raghavan, *Bioresour. Technol.*, 2012, **110**, 214–218.

90 A. Cereda, A. Hitchcock, M. D. Symes, L. Cronin, T. S. Bibby and A. K. Jones, *PLoS One*, 2014, **9**(3), e91484.

91 G. Longatte, F. Rappaport, F.-A. Wollman, M. Guille-Collignon and F. Lemaître, *Electrochim. Acta*, 2017, **236**, 337–342.

92 S.-H. Chang, B.-Y. Huang, T.-H. Wan, J.-Z. Chen and B.-Y. Chen, *RSC Adv.*, 2017, **7**, 56433–56439.

93 Y. Hindatu, M. Annuar and A. Gumel, *Renewable Sustainable Energy Rev.*, 2017, **73**, 236–248.

94 L. Liu and S. Choi, *Lab Chip*, 2017, **17**, 3817–3825.

95 K. Leitner, A. Lerf, M. Winter, J. O. Besenhard, S. Villar-Rodil, F. Suárez-García, A. Martínez-Alonso and J. M. D. Tascón, *J. Power Sources*, 2006, **153**, 419–423.

96 Z. Yang, L. Zhang, C. Nie, Q. Hou, S. Zhang and H. Pei, *Water Res.*, 2019, **164**, 114955.

97 Y. Yan, J. Miao, Z. Yang, F.-X. Xiao, H. B. Yang, B. Liu and Y. Yang, *Chem. Soc. Rev.*, 2015, **44**, 3295–3346.

98 N. Sekar, Y. Umasankar and R. P. Ramasamy, *Phys. Chem. Chem. Phys.*, 2014, **16**, 7862–7871.

99 M. Sawa, A. Fantuzzi, P. Bombelli, C. J. Howe, K. Hellgardt and P. J. Nixon, *Nat. Commun.*, 2017, **8**, 1–10.

100 N. Sekar, R. Jain, Y. Yan and R. P. Ramasamy, *Biotechnol. Bioeng.*, 2016, **113**, 675–679.

101 S. K. Chaudhuri and D. R. Lovley, *Nat. Biotechnol.*, 2003, **21**, 1229–1232.

102 S. N. Mohamed, P. A. Hiraman, K. Muthukumar and T. Jayabalan, *Bioresour. Technol.*, 2020, **295**, 122226.

103 J. Wei, P. Liang and X. Huang, *Bioresour. Technol.*, 2011, **102**, 9335–9344.

104 S. Naina Mohamed, P. Ajit Hiraman, K. Muthukumar and T. Jayabalan, *Bioresour. Technol.*, 2020, **295**, 122226.

105 K. Raman and J. C.-W. Lan, *Appl. Energy*, 2012, **100**, 100–105.

106 L.-F. Huang, J.-Y. Lin, K.-Y. Pan, C.-K. Huang and Y.-K. Chu, *Int. J. Mol. Sci.*, 2015, **16**, 19308–19325.

107 J. C.-W. Lan, K. Raman, C.-M. Huang and C.-M. Chang, *Biochem. Eng. J.*, 2013, **78**, 39–43.

108 J. Liu, Y. Liu, C. Feng, Z. Wang, T. Jia, L. Gong and L. Xu, *Energy Sci. Eng.*, 2017, **5**, 217–225.

109 L. F. Castañeda, F. C. Walsh, J. L. Nava and C. P. de Leon, *Electrochim. Acta*, 2017, **258**, 1115–1139.

110 X.-g. Li, K.-l. Huang, S.-Q. Liu, T. Ning and L.-q. Chen, *Trans. Nonferrous Met. Soc. China*, 2007, **17**, 195–199.

111 K. Nishio, K. Hashimoto and K. Watanabe, *Appl. Microbiol. Biotechnol.*, 2010, **86**, 957–964.

112 K. Nishio, K. Hashimoto and K. Watanabe, *J. Biosci. Bioeng.*, 2013, **115**, 412–417.

113 Q. Cheng, J. Tang, J. Ma, H. Zhang, N. Shinya and L.-C. Qin, *J. Phys. Chem. C*, 2011, **115**, 23584–23590.

114 K. Hasan, H. B. Yildiz, E. Sperling, P. Ó. Conghaile, M. A. Packer, D. Leech, C. Hägerhäll and L. Gorton, *Phys. Chem. Chem. Phys.*, 2014, **16**, 24676–24680.

115 D. Levy and E. Castellón, *Transparent Conductive Materials: Materials, Synthesis, Characterization, Applications*, John Wiley & Sons, 2018.

116 F.-L. Ng, M. M. Jaafar, S.-M. Phang, Z. Chan, N. A. Salleh, S. Z. Azmi, K. Yunus, A. C. Fisher and V. Periasamy, *Sci. Rep.*, 2014b, **4**, 7562.

117 H. Hosono and K. Ueda, in *Springer Handbook of Electronic and Photonic Materials*, ed. S. Kasap and P. Capper, Springer International Publishing, Cham, 2017, p. 1, DOI: DOI: 10.1007/978-3-319-48933-9_58.

118 F. Calignano, T. Tommasi, D. Manfredi and A. Chiolerio, *Sci. Rep.*, 2015, **5**, 17373.

119 A. E. Inglesby, K. Yunus and A. C. Fisher, *Phys. Chem. Chem. Phys.*, 2013, **15**, 6903–6911.

120 J. Yang, DIGITIMES Research, Taipei, Friday 28 December 2012, 2012.

121 K. Ghaffarzadeh, *ITO alternative leaders will emerge despite the pending consolidation*, 2015.

122 J. Meiss, C. Uhrich, K. Fehse, S. Pfuetzner, M. Riede and K. Leo, Society of Photo-Optical Instrumentation Engineers, Proceedings Volume 7002, *Photonics for Solar Energy Systems II*, 2008, vol. 7002, p. 700210.

123 K. Hasan, E. Çevik, E. Sperling, M. A. Packer, D. Leech and L. Gorton, *Adv. Energy Mater.*, 2015, **5**, 1501100.

124 K. Hasan, V. Grippo, E. Sperling, M. A. Packer, D. Leech and L. Gorton, *ChemElectroChem*, 2017, **4**, 412–417.

125 Y. L. Kang, S. Ibrahim and S. Pichiah, *Bioresour. Technol.*, 2015, **189**, 364–369.

126 C. Feng, Z. Lv, X. Yang and C. Wei, *Phys. Chem. Chem. Phys.*, 2014, **16**, 10464–10472.

127 C. Li, L. Zhang, L. Ding, H. Ren and H. Cui, *Biosens. Bioelectron.*, 2011, **26**, 4169–4176.

128 C.-H. Liu, T.-H. Ko, E.-C. Chang, H.-D. Lyu and Y.-K. Liao, *J. Power Sources*, 2008, **180**, 276–282.

129 D. Park and J. Zeikus, *Appl. Microbiol. Biotechnol.*, 2002, **59**, 58–61.

130 K. Scott, G. Rimbu, K. Katuri, K. Prasad and I. Head, *Process Saf. Environ. Prot.*, 2007, **85**, 481–488.

131 O. Lupan, V. Guérin, I. Tiginyanu, V. Ursaki, L. Chow, H. Heinrich and T. Pauporté, *J. Photochem. Photobiol., A*, 2010, **211**, 65–73.

132 D. H. Park and J. G. Zeikus, *Biotechnol. Bioeng.*, 2003, **81**, 348–355.

133 D. A. Lowy, L. M. Tender, J. G. Zeikus, D. H. Park and D. R. Lovley, *Biosens. Bioelectron.*, 2006, **21**, 2058–2063.

134 J. R. Kim, B. Min and B. E. Logan, *Appl. Microbiol. Biotechnol.*, 2005, **68**, 23–30.

135 S. Cheng and B. E. Logan, *Electrochem. Commun.*, 2007, **9**, 492–496.

136 M. Adachi, T. Shimomura, M. Komatsu, H. Yakuwa and A. Miya, *Chem. Commun.*, 2008, 2055–2057.

137 A. L. Popov, J. R. Kim, R. M. Dinsdale, S. R. Esteves, A. J. Guwy and G. C. Premier, *Biotechnol. Bioprocess Eng.*, 2012, **17**, 361–370.

138 Y. Yuan and S.-H. Kim, *Bull. Korean Chem. Soc.*, 2008, **29**, 168–172.

139 N. T. Aboulkhair, M. Simonelli, L. Parry, I. Ashcroft, C. Tuck and R. Hague, *Prog. Mater. Sci.*, 2019, **106**, 100578.

140 M. Y. Teo, L. Stuart, K. Aw and J. Stringer, *NIP & Digital Fabrication Conference*, 2018, **2018**, 16–20.

141 F. Calignano, T. Tommasi, D. Manfredi and A. Chiolerio, *Sci. Rep.*, 2015, **5**, 17373.

142 Y. Zhao, S. Nakanishi, K. Watanabe and K. Hashimoto, *J. Biosci. Bioeng.*, 2011, **112**, 63–66.

143 T. Herling, T. Müller, L. Rajah, J. Skepper, M. Vendruscolo and T. Knowles, *Appl. Phys. Lett.*, 2013, **102**, 184102.

144 S. Malik, E. Drott, P. Grisdela, J. Lee, C. Lee, D. A. Lowy, S. Gray and L. M. Tender, *Energy Environ. Sci.*, 2009, **2**, 292–298.

145 O. Prakash, A. Mungray, S. K. Kailasa, S. Chongdar and A. K. Mungray, *Process Saf. Environ. Prot.*, 2018, **117**, 11–21.

146 L. Zhang, I. Álvarez-Martos, A. Vakurov and E. E. Ferapontova, *Sustainable Energy Fuels*, 2017, **1**, 842–850.

147 Y. Li, Y. Lin, P. C. Loughlin and M. Chen, *Front. Plant Sci.*, 2014, **5**, 67.

148 R. Ramaraj, D. D. Tsai and P. H. Chen, *Chiang Mai J. Sci.*, 2013, **40**, 547–555.

149 N. Samsonoff, M. D. Ooms and D. Sinton, *Appl. Phys. Lett.*, 2014, **104**, 043704.

150 X. Wei, H. Lee and S. Choi, *Sens. Actuators, B*, 2016, **228**, 151–155.